AD-A043 405 GENERAL RESEARCH CORP SANTA BARBARA CALIF F/G 17/8
TARGET ACQUISITION WITH FLIR AND TV (A DESCRIPTION OF COMPUTER --ETC(U)
SEP 76 H F GILMORE, A D STATHACOPOULOS F33615-76-C-0116
UNCLASSIFIED CR-1-732 NL

1 OF 1
AD A043405

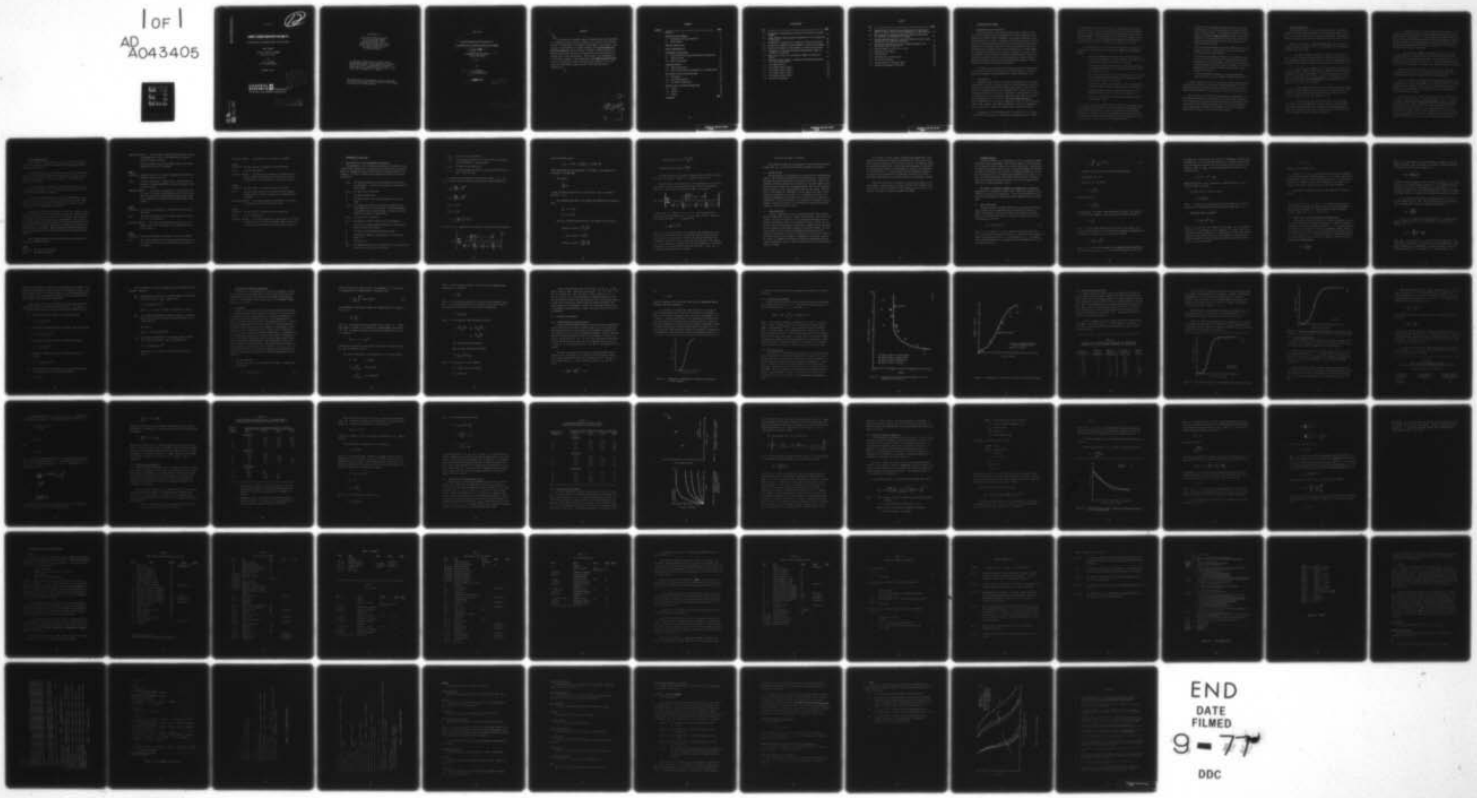

END
DATE FILMED
9-77
DDC

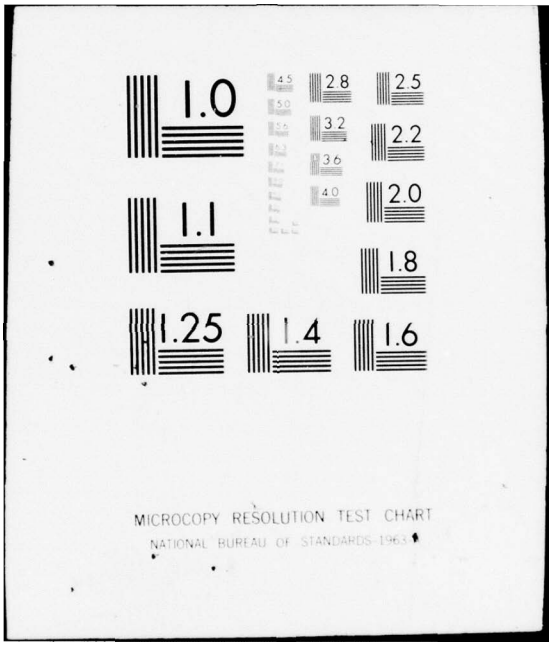
1.0
1.1
1.25
1.4
1.6
1.8
2.0
2.2
2.5
2.8
3.2
3.6
4.0
4.5
5.0
5.6
MICROCOPY RESOLUTION TEST CHART
NATIONAL BUREAU OF STANDARDS-1963-A

CR-1-732

TARGET ACQUISITION WITH FLIR AND TV

(A DESCRIPTION OF COMPUTER CODES IOTA AND OBOE)

FINAL REPORT

Contract F33615-76-C-~~0166~~ 0116
Project No. A325

by

H. F. Gilmore
A. D. Stathacopoulos

September 1976

GENERAL RESEARCH CORPORATION
P.O. BOX 3587, SANTA BARBARA, CALIFORNIA 93105

Sponsored by

Aeronautical Systems Division
Air Force Systems Command
United States Air Force
Wright-Patterson AFB, Ohio 45433
Under Contract F33615-76-C-0116,
Item 0001, Sequence No. 4
Project No. A325

In addition to approval by the Project Leader and Department Head, General Research Corporation reports are subject to independent review by a staff member not connected with the project. This report was reviewed by C. J. Landry.

CR-1-732

TARGET ACQUISITION WITH FLIR AND TV

(A DESCRIPTION OF COMPUTER CODES IOTA AND OBOE).

FINAL REPORT

Contract F33615-76-C-0116

Project No. A325

by

H. F. Gilmore
A. D. Stathacopoulos

September 1976

79p.

ABSTRACT

The acquisition of ground targets by airborne observers using FLIR or TV sensors involves a series of steps, one of which is the actual detection or recognition of the target on the display of the sensor. This process is represented by a computer program, IOTA (**Infrared-Observer-Television Analysis**), which contains a flexible, detailed model of the sensor system itself and which also provides for the representation of unaided visual target acquisition. IOTA contains a new formulation of the observer's response. This formulation, OBOE (**OBserver-Optical Equations**), is described in detail and calculations made with it are compared with experimental results and with other display-observer formulations.

CONTENTS

ILLUSTRATIONS

TABLES

1 INTRODUCTION AND SUMMARY

1.1 BACKGROUND AND STUDY OBJECTIVE

The work reported on here was performed at GRC in support of the US Air Force Mission Analysis on Offensive Air Support conducted at the Aeronautical Systems Division (ASD/XRO). The target acquisition portion of the ASD study is, in part, concerned with the effectiveness of electro-optical (E-O) sensors and their operators in performing real-time target acquisition from airborne platforms. Selecting appropriate analytical representations or models of E-O sensors and operators for such a study is a complex and difficult task for several reasons: The present state of knowledge of all the factors involved in representing E-O sensors and observers is limited; none of the current models use all the presently available knowledge; and the various existing models emphasize different aspects of E-O sensor and operator performance.

Accordingly, the objective of this study was to select appropriate state-of-the-art analytic formulations of the performance of E-O sensors and their operators in performing specific target acquisition tasks.

1.2 STUDY RESULTS

Originally, this study was to select an appropriate set of analytic formulations for ASD's use from the 1976 E-O sensor modeling survey[1] made by GRC for the Target Acquisition Working Group (TAWG). After further review of available models, it was concluded that (1) none of the existing models contained a sufficiently comprehensive representation of operator performance (static and dynamic aspects) and (2), from the available multisensor models (TV, FLIR, etc.), only GRC's GAMMA and the Air Force's MARSAM models were directly applicable to the E-O sensor representation task. However, both GAMMA and MARSAM are much more comprehensive than is required to simulate the dynamic target acquisition sequence.

Consequently, it was determined that the objectives of the current study would be best met by (1) assembling a condensed version of GAMMA

to represent E-O sensors (TV, FLIR) and (2) formulating a new observer performance model. This new formulation treats both static and dynamic aspects of target acquisition and is more comprehensive than currently available models. It is applicable to both TV and FLIR sensors as well as the unaided eye because it emphasizes in appropriate fashion the related factors of contrast, resolution, and signal-to-noise ratios.

The representations of E-O sensors finally chosen, as well as the overall model framework, were abstracted from GAMAA by the following steps:

1. Portions of GAMMA--those used for other sensors such as vertical IR, photography, etc.--were deleted. The remainder was sufficient to model FLIR, TV, and LLTV sensors.

2. Various modifications were made to the remaining subroutines to simplify and shorten them, sacrificing some input flexibility for ease of use.

3. The required input format was made simpler than that in GAMMA, since eliminating unneeded portions of the program relaxed the input requirements considerably.

4. A new routine, AIRFLY, was prepared to fly the sensor-bearing aircraft on input-controlled, point-by-point flight paths.

5. Appropriate modifications were made to account for the eye Modulation Transfer Function (MTF) of the observer.

6. Subroutines were written to represent an airborne observer using unaided vision.

The new observer performance model, called OBOE (for OBserver Optical Equations), uses an empirically derived format, containing factors whose form and parameters were varied and adjusted until reasonable agreement was achieved with selected experimental data and other models. The agreement achieved is quite comprehensive and is presented in Sec. 6 of this report. The key features of the OBOE model are:

1. It can be used to evaluate the human eye as well as sensors operating both in the visible portion of the spectrum (TV) and the infrared (FLIR). Its formulation treats the related effects of displayed **target-background** contrast (especially significant in TV performance), and the overall system resolution and displayed signal-to-noise ratio (important for both TV and FLIR sensors).

2. It shows very good agreement with much experimental data collected under static conditions such as that of Blackwell,[2] Johnson,[3] and Rosell and Willson.[4]

3. It incorporates an empirical term for scene complexity similar to the term used by Bailey,[5] thus permitting a degree of consideration of the performance effects of structured nonuniform backgrounds and their impact on glimpse size and minimum mean time to search the display under dynamic target acquisition conditions.

4. It shows encouraging agreement with existing laboratory search data such as that of Boynton and Bush[6] and Erickson.[7]

To model the dynamic effects of target acquisition including scene and target size changes as the airborne platform approaches the target, appropriate analytical expressions were incorporated for accumulating single glance probabilities as a function of time along the flight path.

The E-O sensor and related subroutines extracted from GAMMA, the OBOE observer performance formulations, the aircraft flight subroutine, and the probability accumulation expressions have been incorporated into a new model, called IOTA (Infrared, Observer, and Television Analysis). IOTA is programmed in FORTRAN IV and designed for static and dynamic comparisons of unaided vision and TV and FLIR sensors.

2 COMPUTER PROGRAM IOTA

IOTA (Infrared, Observer, and Television Analysis) is a computer program for estimating the performance of airborne visual observers and FLIR, TV, and LLTV sensors viewing targets on the ground. The program includes performance calculations of humans observing the sensor display.

IOTA is an outgrowth of GAMMA (Ground-Air Multi-sensor Model A), a program previously developed at GRC.[8] In developing IOTA from GAMMA the following steps were taken:

1. Portions of GAMMA not needed for FLIR, TV, or LLTV sensors were not used. GAMMA contains provisions for modeling vertical IR sensors, photography, direct viewing devices, TV sensors using storage tubes, and active visible sensors; these capabilities were not included in IOTA.

2. Only one part of GAMMA's overall display-observer representation was retained. (GAMMA contains what are essentially three independent formulations of observer performance.) The most versatile set of equations, developed during work on this contract, was incorporated into IOTA. This set of equations (called OBOE--OBserver Optical Equations) is discussed in Secs. 5 and 6 of this report.

3. Various modifications were made to shorten and simplify GAMMA subroutines. While GAMMA was written to accept a great variety of input options, doing so provides great flexibility at the expense of code length. We removed most of these options for IOTA.

4. The input format and the required inputs were simplified. The flexibility of the GAMMA input options results in a rather complicated input format; reducing this flexibility and eliminating the portions of the program not necessary to represent FLIR, TV, and LLTV sensors considerably relaxed the input requirements.

5. A number of blocks of code were written, including (1) an executive subroutine (AIOTA) that provides a bridge between the input data and the rest of the program, (2) a control subroutine (AIRFLY) that moves the sensor along a flight path composed of arbitrary straightline segments, and (3) an addition to the OBserver Optical Equations (OBOE) that allows cummulative probabilities of detection and recognition to be obtained as the sensor moves along a flight path.

6. New subroutines (EYERSP and VISUAL) were written to permit the representation of unaided visual observation within the same basic structure used for electro-optical sensors. This representation does not take into account possible effects of color. It thus should be used only when color cues are minimal, a condition very common in military operations.

While the present form of IOTA is a useful tool for analyzing airborne sensors, it is still being improved, and various modifications to increase its versatility and accuracy are being considered.

Since it is derived from GAMMA, IOTA's modeling philosophy and code structure are to a large extent GAMMA's. As a result, some of the coding framework is more elaborate than is strictly necessary for the sensors modeled; on the other hand, this framework allows considerable room for modifications and development.

The overall structure of IOTA includes four classes of subroutines: (1) executive subroutines such as AIOTA and AIRFLY; (2) a set of seven subroutines (TARGET, TARPRO, IRIRRA, CALCWL, PASILL, PASIRR, and EYERSP) that deal with the target, its location, and the atmosphere and calculate effective target irradiance at the sensor aperture; (3) a set of subroutines (discussed in Secs. 3 and 4) represents electro-optical sensors and, correspondingly, aspects of unaided vision; (4) two subroutines (GEOBSV and OBSERV, Secs. 5 and 6) that represent the human observer.

3 SENSOR REPRESENTATIONS

IOTA represents the performance of FLIR, TV, and LLTV sensors by calling, in succession, different subroutines representing the modules that model these sensors.

The module subroutines for the FLIR sensor are OPTICS, which represents the optical systems, DETECT, which represents the detector array, AMPFY2, which represents the electronic amplifier, and TVDISP, which represents the display.

For TV, the module subroutines are OPTICS, AMPFY1 (which in this case represents the aperture stop), TVCAMA (which represents the television camera tube), AMPFY2, and TVDISP.

For LLTV, the module subroutines are OPTICS, INTENS (which represents photon noise effects in the image intensification process, AMPFY1 (which, in this case, represents the combination of aperture stop and intensifier gain), TVCAMA, AMPFY2, and TVDISP.

In general, these module subroutines calculate (1) resolution degradation, (2) noise, and (3) an input-output relationship, called the amplitude transfer function (some do not provide all three). When a module is responsible for resolution degradation, a gaussian MTF curve is fitted to the module MTF curve, and the variance of the Fourier transform of the gaussian MTF curve is used to represent the variance of the point-spread function (PSF) of the module. Noise is described within the program in terms of its power per unit spatial frequency and its effective spatial bandwidth.

The following paragraphs describe briefly the various module subroutines in alphabetical order.

AMPFY1

Resolution: Not effect on resolution.

Noise: No noise contribution.

Amplitude Transfer: For TV systems, reduces the OPTICS output to match the maximum input level of the TVCAMA when the former is larger; otherwise no effect.

For LLTV systems, increases the INTENS output to match the maximum input level of the TVCAMA.

AMPFY2

Resolution: Degrades resolution to an extent depending on the amplifier bandwidth and the scan rate.

Noise: No noise contribution. (Camera tube or detector noise is assumed to include preamplifier noise and to dominate other electronic noise.)

Amplitude Transfer: The output of this module is a linear function of the input. The linear relationship is set up in such a way that the maximum and minimum background levels will appear on the display at the extremes of the dynamic range of the display.

DETECT

Resolution: The resolution degradation is calculated from the detector dimensions.

Noise: The noise is obtained from the incident power and the spectral D* of the detector.

Amplitude Transfer: The output is proportional to the area of the detector and to the flux density in the image plane of the optical system.

INTENS

Resolution: Resolution degradation is included in that of the TVCAMA.

Noise: The incident radiation levels and the quantum efficiency of the photocathode are used to determine the photon noise in the output.

Amplitude Transfer: This property is accounted for in AMPFY1.

OPTICS

Resolution: The PSF variance is computed from the module MTF.

Noise: No noise contribution.

Amplitude Transfer: The image plane irradiance is computed from the object radiance as modified by the focal ratio, and the atmosphere and the transmittance of the optical system.

TVCAMA

Resolution: The PSF variance is computed from the module MTF.

Noise: The noise power spectrum is determined from the maximum signal-to-noise ratio of the tube and the maximum cathode irradiance.

Amplitude Transfer: The output voltage is proportional to the input irradiance up to the tube saturation level.

TVDISP

Resolution: The PSF variance is computed from the module MTF.

Noise: No noise contribution.

Amplitude transfer: The output brightness is proportional to the input voltage but must lie within the dynamic range of the display as specified by the maximum and minimum output brightness.

4 PERFORMANCE CALCULATIONS

4.1 ELECTRO-OPTICAL SYSTEM PERFORMANCE CALCULATIONS

The performance of the electro-optical system is calculated in subroutine SYSCAL through a set of equations which yield various quantities useful for comparing different systems and for estimating observer performance. In order to describe these equations we will use the following notation.

$(\sigma_x)_i$ The standard deviation in the x-direction of the PSF of the ith module. The units are fractions of the frame (or field) width.

$(\sigma_y)_i$ The same in the y-direction.

F The display width, feet.

N_i The noise power per unit spatial frequency of the ith stage.

$(\eta_x)_i$ The standard deviation of the Fourier transform of the noise bandwidth in the x-direction. The noise bandwidth is assumed to have a Gaussian shape. The units are fractions of the frame (or field) width.

$(\eta_y)_i$ The same in the y-direction.

$T_i(\ )$ The amplitude transfer function for the ith module.

T The effective target radiance (taking into account atmospheric effects) at the sensor.

B The same for the background around the target.

D_T The display brightness corresponding to a system input equal to T.

D_B The same for B.

$(\sigma_x)_T$ The standard deviation of the overall PSF in the x-direction divided by the frame (or field) width.

$(\sigma_y)_T$ The same in the y-direction.

$(\hat{\sigma}_x)_T$ The standard deviation of the overall PSF on the display in the x-direction. Units are feet.

$(\hat{\sigma}_y)_T$ The same in the y-direction.

$\hat{\sigma}_T$ The mean standard deviation of the overall PSF on the display. Units are feet.

In computing the performance of the overall system, $(\sigma_x)_T$ and $(\sigma_y)_T$ are first obtained from the individual PSF standard deviations:

$$(\sigma_x)_T = \left(\sum_i (\sigma_x)_i^2\right)^{1/2}$$

$$(\sigma_y)_T = \left(\sum_i (\sigma_y)_i^2\right)^{1/2}$$

$$(\hat{\sigma}_x)_T = (\sigma_x)_T F$$

$$(\hat{\sigma}_y)_T = (\sigma_y)_T F$$

$$\hat{\sigma}_T = \frac{1}{\sqrt{2}} \sqrt{(\hat{\sigma}_x)_T^2 + (\hat{\sigma}_y)_T^2}$$

The RMS noise N_R appearing on the display is evaluated from the equation

$$N_R = \left[\sum_i \frac{N_i \prod_{i+1}^{n} \left(\frac{dT_j}{dx} \,\middle|\, T_{j-1},\ldots,T_1(B)\right)^2}{4\pi \sqrt{(\eta_x)_i^2 + \sum_{i+1}^{n} (\sigma_x)_j^2} \sqrt{(\eta_y)_i^2 + \sum_{i+1}^{n} (\sigma_y)_j^2}}\right]^{1/2}$$

Here the notation used is

$$T_{j-1},\ldots,T_1(B) = T_{j-1}\left(T_{j-2}\left(\ldots(T_1(B))\right)\ldots\right)$$

These expressions give the amplitude of the image of the background at the input to the jth stage.

The notation

$$\frac{dT_j}{dx}\Big|_{x_1}$$

is used to denote the derivative of the function $T_j(x)$ evaluated at the point $x = x_1$.

The displayed amplitudes of the target and background are calculated from

$$D_B = T_n\ldots T_1(B)$$

$$D_T = T_n\ldots T_1(T)$$

Then the following characteristics of the display are calculated:

$$\text{Displayed contrast} = \frac{|D_T - D_B|}{D_B}$$

$$\text{Input contrast} = \frac{|T - B|}{B}$$

$$\text{Contrast transfer} = \frac{B(D_T - D_B)}{D_B(T - B)}$$

$$\text{Signal-to-noise ratio} = \frac{\left|D_T - D_B\right|}{N_R}$$

$$\text{Limiting cycles per frame} = \frac{0.225F}{\hat{\sigma}_T}$$

Here the constant 0.225 yields a frequency where the MTF corresponding to the PSF having a variance $\hat{\sigma}_T$ is down by a factor 1/e.

The next step in the calculation is the determination of the smoothing required to make the signal-to-noise ratio equal to the arbitrary value of 2. This is done in subroutine SFINDR. The equation

$$\left|D_B - D_T\right| = 2\left\{\sum_i \frac{N_i \prod_{i+1}^{n} \left[\frac{dT_j}{dx} \left| T_{j-1} \cdots T_1(B)\right.\right]^2}{4\pi \sqrt{(\eta_x)_i^2 + \sum_{i+1}^{n} (\sigma_x)_j^2 + S^2}\sqrt{(\eta_y)_i^2 + \sum_{i+1}^{n} (\sigma_y)_j^2 + S^2}}\right\}^{1/2}$$

is solved for S. (However, if, for $S = 0$, the left-hand side is greater than the right-hand side, S is set equal to zero.) Then a new PSF standard deviation σ^* is computed from

$$\sigma_T^* = \sqrt{\hat{\sigma}_T^2 + (SF)^2}$$

where F is the display width. This composite PSF combines the actual blur of the system with the blur necessary to make the signal-to-noise ratio equal to 2 and is used to represent the spatial integration the eye makes to observe the target in the noise that appears on the display. σ_T^* can be considered to represent the effective resolution of the display taking into account both display resolution and noise. Using σ_T^*, a limiting frequency response is obtained:

$$\sigma_T^* \text{ (cycles per frame)} = 0.225F/\sigma_T^*$$

These computed quantities are provided as output, and the displayed contrast and σ_T^* are used in the observer performance calculation.

4.2 UNAIDED VISION

The performance of the unaided eye is calculated by assigning proper values to the variables discussed in the previous section. The procedure describes an observer searching a fixed area on the ground. Within the program an artificial display is set up which is just big enough to encompass this area, and which has unit magnification; that is, the displayed target subtends the same visual angle as does the real target. The contrast of this display is considered to be the same as the input contrast (taking the atmosphere into account); it is noiseless, and there is no resolution degradation (except that due to the eye; this is introduced subsequently). With this artifact, the calculation of unaided visual performance is exactly the same as the calculation of display observer performance, discussed in Secs. 5 and 6.

4.3 OTHER SUBROUTINES

In IOTA, characteristics of the target that affect sensor performance are taken into account in a number of subroutines. For TV and LLTV sensors, the spectral reflectance of the target and background and the incident illumination level in foot-candles are inputs. Within the program the spectral distribution of the incident illumination is calculated (this is assumed to approximate sunlight) in subroutine CALCWL, and then this, together with the target and background reflectances and the response of the sensor, are used to calculate what the effective input to the sensor would be in the absence of atmospheric scattering. Finally, the effect of atmospheric scattering in reducing target-background contrast are taken into account. These calculations are done in subroutines PASILL and PASIRR.

For the FLIR, the input target and background temperatures, their spectral emissivities, the spectral atmospheric extinction coefficients, and the spectral response of the sensor are inputs. In subroutine IRIRRA the aperture irradiances due to the target and background are calculated by integrating the products of the appropriate factors over wavelength. In this calculation it is assumed that spectral atmospheric absorption with range can be represented by exponential functions; this yields a reasonable approximation to total band absorption in atmospheric windows.

Additional calculations of geometric factors must be made for all three sensors. These involve the target position on the display screen, calculated in subroutine TARGET, and the dimensions of the target on the display, calculated in subroutines TARPRO and GEOBSV.

5 OBSERVER MODELING

In IOTA the observer is represented by a set of calculations (OBOE) performed in subroutine OBSERV. The principal inputs to this subroutine can be classed as either geometrical or sensor descriptors. The geometrical inputs are obtained from the output of subroutine GEOBSV, and include the area of the target on the display, the minimum dimension of the target on the display, and the average angle subtended by the target at the eye. The sensor descriptors are obtained from the output of subroutine SYSCAL and include the standard deviation of the sensor composite PSF (σ_T^*) and the target-background contrast.

The outputs of subroutine OBSERV are probabilities of detection, probabilities of recognition, display search times, and cumulative probabilities of detection and recognition. These various probabilities and times will be discussed in connection with the equations used to compute them.

5.1 OBOE CALCULATIONS

The main portion of the OBOE calculation is concerned with obtaining an estimate of the probability that an observer will detect, or detect and recognize, a particular target on the display in a single glance. The procedure followed is to compute a signal index (SI) from an expression of the form

$$SI = \{F_1 \cdot F_2 \cdot F_3 \cdot F_4\}^{1/2} \tag{5.1}$$

where F_1 is a constant, F_2 is a function of resolution and noise, F_3 is a function of target contrast, and F_4 depends on scene complexity. Using a fixed threshold level L, the difference $SI - L$ is computed, and the desired probability is computed from an approximation to the common gaussian integral

$$P = \int_{-\infty}^{SI-L} \frac{1}{\sqrt{2\pi}} e^{-x^2/2} \, dx \qquad (5.2)$$

In OBOE, the various factors have the following forms.

The constant $F_1 = 160$

The factor F_2 is given by

$$F_2 = \frac{N^2}{N^2 + 10}$$

for detection and by

$$F_2 = \frac{N^2}{N^2 + 100}$$

for recognition. (We denote these expressions by $F_2(10)$ and $F_2(100)$.) N is the effective number of lines across the target and is given by

$$N = \frac{M}{\sqrt{2\pi}\sigma}$$

where M is the minimum dimension of the target on the display, and σ is the standard deviation of the overall PSF, including, when appropriate, the effects of the human eye. We use the relationship

$$\sigma = \left(\sigma_T^{*2} + \sigma_E^2\right)^{1/2}$$

where σ_T^* is the standard deviation of the composite point spread function described earlier and σ_E is the standard deviation of the PSF of

the human eye. We have found that results of experiments on human vision, discussed in Sec. 6, can best be matched if σ_E represents the distance on the display which subtends about 0.4 minutes of arc at the eye of the observer. Thus, if R_{OBS} is the distance between the observers' eye and the display,

$$\sigma_E = 1.16 \times 10^{-4} \times R_{OBS}$$

When modeling purely visual observation, as mentioned above, $\sigma_T^* = 0$ since no sensor is involved.

The third factor is given by either

$$F_3 = \frac{C}{0.9C + 0.1}$$

where C is equal to the displayed contrast described in the previous section, or, if the displayed contrast is greater than unity, $F_3 = 1$.

The fourth factor is given by

$$F_4 = \frac{A_T}{KA_G + (1 - K)A_T}$$

where A_T is the area of the target on the display, A_G is the glance area, and K is a measure of scene complexity. The glance area is the area on the display encompassed in a single glance; in the human observer theories on which OBOE is based, this is thought to be adjusted automatically within the observer depending on display and target characteristics. A_G always satisfies

$$A_T \leq A_G \leq A_D$$

where A_D is the display area.

The use of K in F_4 is rather arbitrary, and future validation of this form will involve relating values of K to various types of displayed terrain scenes. We have found that values of K on the order of 0.001 seem to represent scenes of low complexity, while values on the order of 0.02 seem to represent scenes of very high complexity.

Returning to the OBOE calculations, the threshold value used in OBOE is

$$L = 4$$

It can be seen that F_2, F_3, and F_4 are all less than or equal to unity; as the resolution gets worse, or the contrast becomes smaller, or the complexity increases, SI becomes smaller. When the product $F_2 \cdot F_3 \cdot F_4$ equals 0.1, $SI = 4$, and $P = 0.5$.

5.2 SEARCH TIMES AND THE ACCUMULATION OF PROBABILITIES

The observer searches a display in a series of fixations, each taking about one-fourth to one-third of a second. In OBOE, each fixation encompasses an area of the display denoted by A_G. It can be shown that if the display is searched in a series of independent glances randomly distributed over the display, and the probability of detecting the target on a single glance is P, the mean time to search, MTS, which would be the average time to find the target if a number of identical tests were made, can be approximated by

$$MTS = \frac{A_D}{3A_G}\left(\frac{1}{P}\right)$$

where A_D is the display area, and each glance is assumed to take one-third of a second. When the display is searched in a quasi-uniform way, the mean time for search can be shown to be

$$MTS = \frac{A_D}{3A_G}\left(\frac{2 - P}{2P}\right)$$

In OBOE, this latter equation is used. Within the program A_G is varied; for each A_G the single glance probability P is calculated from Eqs. 5.1 and 5.2, and MTS is calculated from the above equation. A_G is adjusted to minimize MTS ; this minimum mean time to search is provided as an output, and it is assumed that the display is searched in this way.

If P_T denotes the probability calculated from Eqs. 5.1 and 5.2 for this minimum value of MTS , the probability that the target will be seen on a single glance placed at random on the display is

$$P_{SG} = P_T\left(\frac{A_G}{A_D}\right)$$

If P_{SG} is calculated as described above for K different times spaced one-third second apart, the probability of detection after K glances, P_K , is

$$P_K = 1 - \prod_{i=1}^{K}\left(1 - P_{SGi}\right)$$

where P_{SGi} is the value of P_{SG} calculated for the ith glance. This accumulation of probabilities is based on the interpretation that single glance probabilities are independent from glance to glance and can be meaningfully applied to the performance of a single observer. As an

alternate interpretation, single glance probabilities may be taken as the fraction of the population which can detect or recognize the target. This interpretation leads to a different procedure for accumulating probabilities. However, only under unusual conditions is there a significant difference between the accumulated probabilities.

In the output of IOTA five probabilities are printed; these differ in the factors used to calculate the signal index SI . The values of SI together with the names we attach to the resulting probabilities are

P_1 : Detection probability based on resolution and noise:

$$SI = \{F_1 \cdot F_2(10)\}^{1/2}$$

P_2 : Detection probability based on resolution, noise, and contrast:

$$SI = \{F_1 \cdot F_2(10) \cdot F_3\}^{1/2}$$

P_3 : Recognition probability based on resolution and noise:

$$SI = \{F_1 \cdot F_2(100)\}^{1/2}$$

P_4: Recognition probability based on resolution, noise, and contrast:

$$SI = \{F_1 \cdot F_2(100) \cdot F_3\}^{1/2}$$

P_5 : Detection based on resolution, noise, and contrast followed by recognition based on resolution and noise:

$$P_5 = P_2 \cdot P_3$$

In the accumulation of glance probabilities three probabilities are obtained. These are:

P_{K1} : The cumulative probability of detection based on resolution, noise, and contrast: P_{SGi} computed from

$$SI = \{F_1 \cdot F_2(10) \cdot F_3 \cdot F_4\}^{1/2}$$

where A_G is chosen to minimize the mean time to search.

P_{K2} : The cumulative probability of detection based on resolution, noise, and contrast, followed by recognition based on resolution and noise:

$$P_{K2} = P_{K1} \cdot P_3$$

where P_3 was described above.

P_{K3} : The cumulative probability of recognition based on resolution, noise, and contrast: P_{SGi} is computed from

$$SI = \{F_1 \cdot F_2(100) \cdot F_3 \cdot F_4\}^{1/2}$$

where again A_G is chosen to minimize the mean time to search.

6 VALIDATION OF THE OBOE CALCULATIONS

Since OBOE is a new formulation of observer performance, a number of comparisons of results with those of other observer models and with experimental results were made during its development and subsequent checkout. The fundamental results which bear on the validity of OBOE appear in this section.

6.1 PHILOSOPHY

Inspection of both existing observer models and many measurements of visual performance suggests that as one parameter (such as resolution or contrast) is varied, the probability of successful performance of a visual task follows an S-shaped curve that is well-represented by a gaussian integral having the general form suggested by Eq. 5.2. Previous GRC studies suggested that for a wide variety of visual detection and recognition tasks such variations in probability of performance could be related to a set of equations in which a signal index is computed and Eq. 5.2 is used to calculate performance probabilities. The general form of the OBOE calculations thus is based on past experience showing that the various factors influencing target detection, namely sensor display and eye resolution, displayed noise, target-background contrast, and scene complexity, can be conveniently represented using the format shown. Having selected this format, the various factors F_1, F_2, F_3, and F_4 were adjusted in form, and the various constants were varied until reasonable agreement with other models and selected experimental data was achieved.

6.2 THE OBOE EQUATIONS

We repeat here the set of equations used in OBOE. A signal index SI is calculated:

$$SI = \{F_1 \cdot F_2 \cdot F_3 \cdot F_4\}^{1/2} \tag{6.1}$$

where the factors are defined below. The probability P of detection or recognition (on a single glance) is calculated from

$$P = \frac{1}{\sqrt{2\pi}} \int_{-\infty}^{SI-4} \exp(-x^2/2)\, dx \qquad (6.2)$$

The probability of detecting a target in a single glance at a display of area A_D is

$$P_{SG} = \frac{A_G}{A_D} \cdot P$$

where A_G is the glance area which appears in the factor F_4. If display search is assumed to be conducted in a random manner, the probability P(T) of target detection or detection and recognition in a time T is given by

$$P(T) = 1 - (1 - P_{SG})^{3T}$$

assuming that each glance occupies about one-third of a second and that P_{SG} does not change in time T.

The factors appearing in the expression for SI are as follows:

$F_1 = 160$ a constant

$F_2 = \frac{N^2}{N^2 + 10}$ for detection

$= \frac{N^2}{N^2 + 100}$ for recognition

Here N is the "effective number of lines" across the minimum target dimension; N is given by

$$N = \frac{M}{\sqrt{2\pi}\sigma}$$

where M is the minimum dimension of a more-or-less rectangular target, and σ is the standard deviation of the system overall PSF including the effects of the observer's eye and noise on the display.

$$F_3 = \frac{C}{0.9C + 0.1}$$

where C is the apparent target-background contrast:

$$C = \frac{|D_T - D_B|}{D_B} \quad \text{for} \quad \frac{|D_T - D_B|}{D_B} \leq 1$$

$$C = 1 \quad \text{for} \quad \frac{|D_T - D_B|}{D_B} > 1$$

D_T = displayed target brightness

D_B = displayed background brightness

$$F_4 = \frac{A_T}{KA_G + (1 - K)A_T}$$

where K is a measure of scene complexity

A_T = target area on the display

A_G = glance area

It will be observed that each of the factors F_2, F_3, F_4 is less than or equal to unity. When they are all unity, SI = 12.6 and P in Eq. 6.2 is almost one. When the product $P_2P_3P_4$ equals 0.1, SI = 4 and P in Eq. 6.2 is 0.5; this represents a threshold condition. Note that the various constants have not been specified to many decimal places; we feel that in view of the great variability between observers, the great variations in experimental results, and the present limited state of knowledge of human responses, attempts at greater precision would not be warranted.

6.3 VALIDATION COMPARISONS

6.3.1 Visual Resolution--Snellen Letters

We have found that OBOE represents satisfactorily many experimental results in which the principal resolution limit is due to the human eye. As mentioned earlier, in representing such experiments we suppose that the resolution of the eye can be represented roughly as having a gaussian PSF with a standard deviation of about 0.4 arc-minutes. Since 0.4 is close to the reciprocal of $\sqrt{2\pi}$, it can be seen that when system resolution is limited by the eye and there is no displayed noise, we can set N equal to M in the expressions for F_2, when M is expressed in arc-minutes.

With this convention we can calculate visual performance against Snellen letters and Landolt C's. People with normal vision recognize these letters when they subtend about 5 minutes of arc.[9] Setting N = 5 in the expression for F_2 (for resolution), and with F_3 and F_4 = 1 gives

$$SI = \left\{160 \times \frac{25}{125}\right\}^{1/2} \approx 5.66$$

and

$$P = 0.95$$

Thus this represents the point where OBOE predicts **recognition ability starts to fall away from unity.**

It is necessary in considering human perception to distinguish between threshold performance, where the probability of performance is about 0.5, and useful performance, where the level of performance is 0.9 or greater. Generally, when subjects are operating at threshold conditions they have the feeling that they are merely guessing. Figure 6.1 shows the probability of recognition plotted against the angular diameter of objects, which may be taken as Snellen letters or Landolt C's. It can be seen that, when the objects subtend 6 arc-minutes, the probability of recognition is essentially unity; when they subtend as little as 3.3

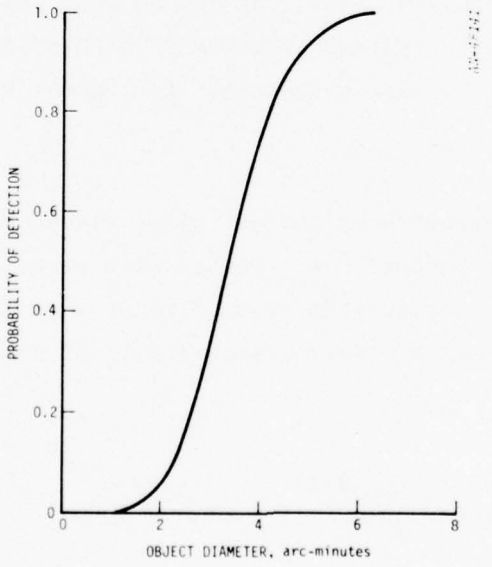

Figure 6.1. Probability of Recognition of Objects as a Function of Object Diameter

arc-minutes, they are essentially unrecognizable--probability of recognition 0.50.

6.3.2 Size-Contrast Threshold

We may calculate the size-contrast relations required for threshold object detection by setting $F_4 = 1$, using the detection expression for F_2, and requiring that $SI = 4$. This gives

$$F_1F_2F_3 = 160 \times \frac{M^2}{M^2 + 10} \times \frac{C}{0.9C + 0.1} = 16$$

where M is the object diameter, in minutes of arc, and C is the contrast. Figure 6.2 shows a plot of this relationship, together with a number of measurements.[2,10] The curve represents the data reasonably well. For large targets, the threshold contrast is about 0.01. Note that threshold detection for contrasts much lower than this are achieved only with very long search times. For small targets the contrast should, on theoretical grounds, be inversely proportional to target area. While this quality is not a property of OBOE, it is not felt to be a drawback since we consider only values of contrast less than or equal to unity.

6.3.3 Relative Contrast

One result of the measurements by Blackwell of the contrast thresholds of the human eye was the observation that the shapes of the curves giving probability of detection as a function of relative contrast (i.e., contrast divided by threshold contrast) was nearly independent of target size.[2] Figure 6.3 shows the average probability curve redrawn from Blackwell, together with plotted points for two size targets calculated from OBOE. The points shown for the 10-minute object represent well all targets larger than about 3 minutes. (It should be noted that in the experiments in question the smallest target subtended 3.60 minutes of arc.)

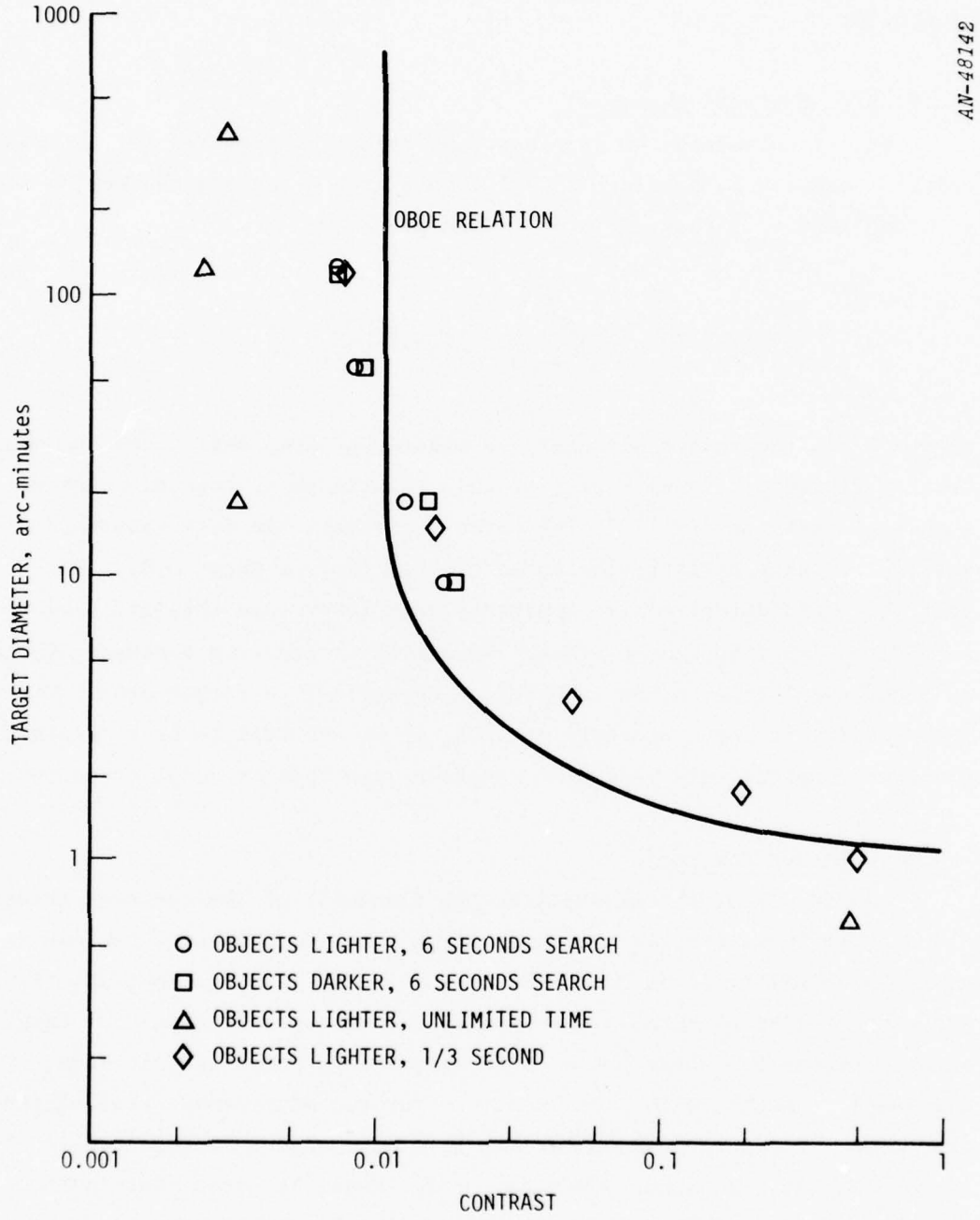

Figure 6.2. Target Diameter Versus Contrast Required for a 0.5 Probability of Detection

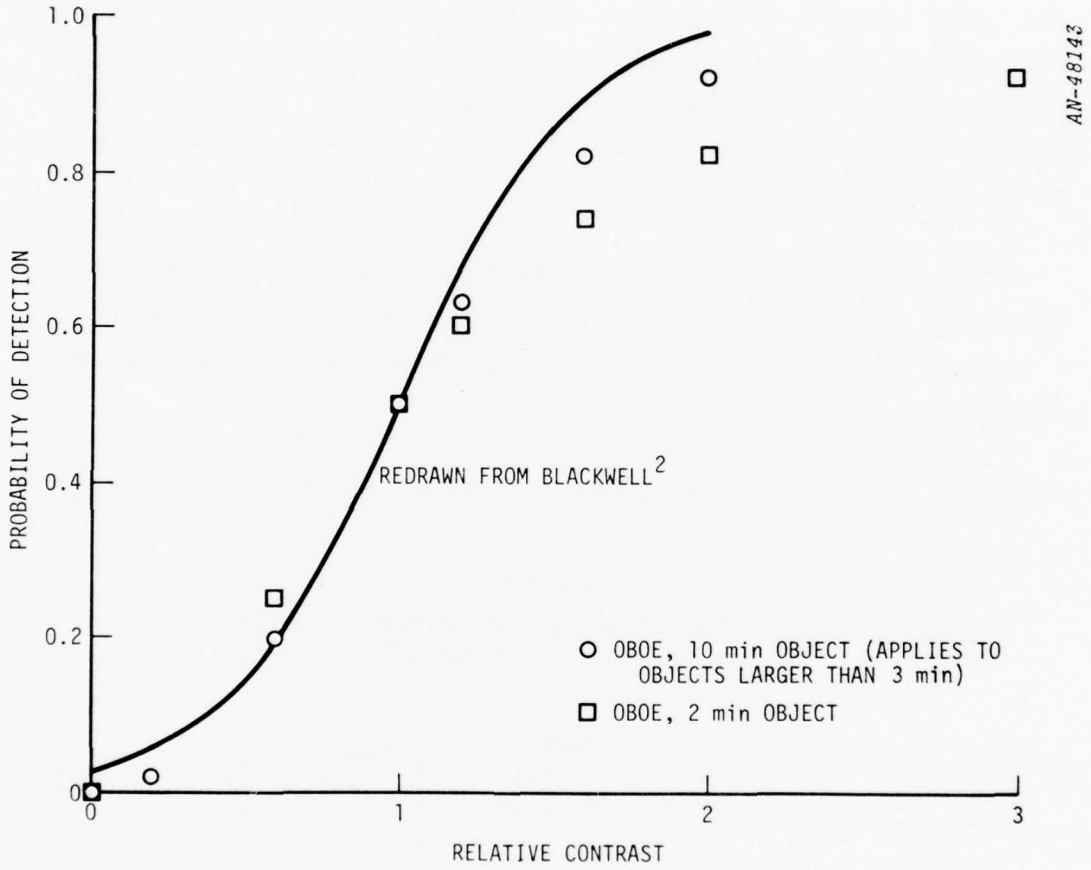

Figure 6.3. Probability of Detection as a Function of Relative Contrast

6.3.4 Sensor Resolution Criteria

A central concept of current theories concerning the detection of military objects was provided by Johnson,[3] who found that the probabilities of detecting and recognizing objects is a rather consistent function of the number of cycles resolvable across a critical dimension of the target. (The critical dimension is the narrowest dimension of the target if the target is more or less rectangular and not too narrow.) Table 6.1 gives probabilities of detection and probabilities of recognition as a function of the number of resolvable cycles. (Two possible relations are shown for recognition probability.)

In order to compare the table to OBOE calculations, we must relate the number of resolvable cycles to N which appears in expression F_2. To do this we draw an analogy between unaided human vision and sensor-aided human vision.

TABLE 6.1

PROBABILITIES OF DETECTION AND RECOGNITION AS A FUNCTION OF NUMBER OF CYCLES ACROSS CRITICAL DIMENSIONS FOR ARMY VEHICLES

Probability of Recognition	Number of Cycles, Relation A	Number of Cycles, Relation B	Probability of Detection	Number of Cycles
1.0	12	9	1.0	3
0.95	8	6	0.95	2
0.80	6	4.5	0.80	1.5
0.50	4	3	0.50	1
0.30	3	2.25	0.30	0.75
0.10	2	1.5	0.10	0.50
0.02	1	0.75	0.02	0.25
0	0	0	0	0

As just described, OBOE represents unaided vision fairly well when N is equal to the target diameter in minutes. A number of measurements have been made of the smallest grid spacing visible to observers. Senders[11] cites the results of six such measurements; the mean is very close to 1 arc-minute. Hence, for the eye, the number of resolvable cycles across a target is equal to N.

We extend this to sensor-aided performance, and suppose that the same relation holds; thus we take N, in the expression for F_2, as representing the number of resolvable cycles across the target.

Figure 6.4 shows the OBOE probability of recognition as a function of the number of resolvable cycles and also the points representing the two relations given in Table 6.1. Figure 6.5 shows the same for detection. In both cases the agreement is satisfactory.

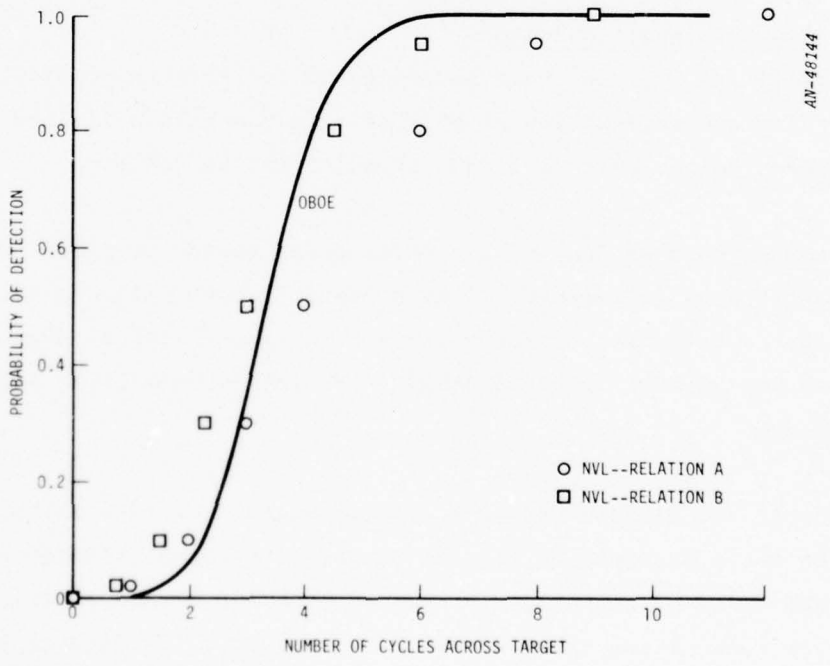

Figure 6.4. Recognition Probability Versus Number of Cycles Across Target

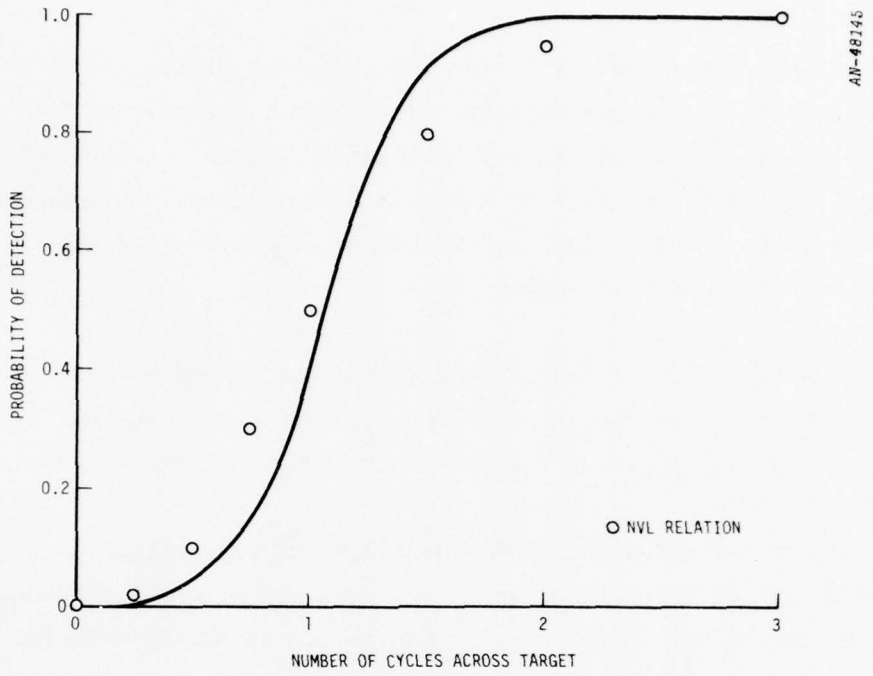

Figure 6.5. Detection Probability Versus Number of Cycles Across Target

6.3.5 Display Signal-to-Noise

Rosell and Willson[4] have investigated the effects of display noise on detection and recognition of objects. We can make a limited comparison between their results and OBOE calculations as follows.

Suppose that we deal with a rectangular target of width M and a target-background difference Δ on a display where noise is the only limitation to detection or recognition. For simplicity we suppose that the noise has a power spectral density W out to relatively high frequencies.

Rosell and Willson define a display signal-to-noise ratio, which, under the above assumptions, is the target-background difference divided by the RMS value of the noise integrated over a fraction of the target area. For recognition the fraction is one-eighth; for detection it is unity.

When wide-band spatial noise having a spectral density W is integrated over an area A, the resulting RMS noise is simply $[W/A]^{1/2}$. If the rectangle has a 2:1 aspect ratio, which is characteristic of the targets Rosell and Willson consider, its area is $2M^2$, and the display signal-to-noise ratio $(SNR)_D$ is thus

$$(SNR)_D = \frac{M\Delta}{2W^{1/2}}$$

for recognition, since the integration area is one-eighth of the target area, and

$$(SNR)_D = \frac{\sqrt{2}M\Delta}{W^{1/2}}$$

for detection, when the integration area is the entire target area. Table 6.2 presents threshold values of $(SNR)_D$ given by Rosell and Willson for detection and recognition of images of military targets on uniform backgrounds. (Their data covers a range of target sizes; that in Table 6.2 is for the two smaller targets.)

To compare these results with OBOE calculations we will determine threshold values of W for the given rectangular target and calculate the corresponding values of $(SNR)_D$.

TABLE 6.2

BEST ESTIMATE OF THRESHOLD DISPLAYED
SIGNAL-TO-NOISE RATIO FOR DETECTION AND RECOGNITION OF IMAGES

(Extracted from Ref. 4; Table 5.6)

Discrimination Level	TV Lines/Minimum Dimension	Threshold (SNR) for Small Targets
Detection	1	2.8
Recognition	8	2.5

In the OBOE equation for SI , we set $F_3 = F_4 = 1$, supposing that the target has high contrast. For threshold recognition we have then

$$160 \frac{N^2}{N^2 + 100} = 16$$

or

$$N = 3.33$$

where

$$N = \frac{M}{\sqrt{2\pi}\sigma}$$

and σ is chosen so that when the noise is integrated over the gaussian blur having the standard deviation σ , the signal-to-RMS noise ratio is equal to 2. We denote this value of σ by S . The RMS noise R obtained in this way is

$$R = \left\{ W \iint \left| e^{-2\pi^2 S^2 \left(R_1^2 + R_2^2\right)} \right|^2 dk_1 dk_2 \right\}^{1/2}$$

$$= \frac{1}{2S} \left(\frac{W}{\pi}\right)^{1/2}$$

and

$$\Delta \Big/ \left(\frac{1}{2S} \left(\frac{W}{\pi}\right)^{1/2} \right) = 2$$

Combining this expression with the earlier one for N and setting N equal to 3.33 gives, for the recognition threshold

$$\frac{M\Delta}{2W^{1/2}} = 2.36 = (SNR)_D$$

where the left-hand side is the display signal-to-noise ratio of Rosell and Willson. For detection, N must be set equal to 1.054, and we obtain the equation

$$\frac{\sqrt{2}M\Delta}{W^{1/2}} = 2.11 = (SNR)_D$$

where the left-hand side is the display signal-to-noise ratio for detection. It can be seen that under the assumption that the display has high resolution and high contrast, OBOE results are similar to those of Rosell and Willson. As contrast decreases, the $(SNR)_D$ obtained from the OBOE calculations increases; for a contrast of 0.5, $(SNR)_D = 2.49$ for recognition.

6.3.6 Display Search Experiments

Between 1954 and 1958 Boynton and his co-workers conducted an extensive series of experiments on the ability of an observer to find a target object among a large number of confusing objects.[6] Target objects and confusing objects were shapes of uniform brightness on a brighter background. Data are available on the effects of search time, number of confusing objects, object size, and object background contrast on the probability of detection.

Table 6.3 gives an important set of summary results on the relation between contrast, size, number of confusing objects, and search time necessary for a 60% probability of detection. We have compared these results with OBOE calculations on the basis of the following observations and assumptions:

1. In these experiments "detection" required recognition of the target, so we are dealing with recognition.

TABLE 6.3

PERCENT CONTRAST REQUIRED TO ELICIT 60 PERCENT CORRECT TARGET RECOGNITION FOR CONDITIONS INDICATED (FROM REF. 7)

Exposure Time, seconds	Approximate Angle Subtended by Target, arc-minutes			
	12.9	8.1	5.4	4.05
	16 Objects			
3	4.9	16.0	29.0	>100
6	3.9	8.4	23.5	60.0
12	3.5	6.0	18.0	41.0
24	3.0	5.3	15.5	37.0
	64 Objects			
3	16.0	46.0		
6	9.8	29.0	85.0	
12	5.8	11.2	43.0	>100
24	4.6	8.6	27.5	46.0
	256 Objects			
3	>100			
6	66.0	>100		
12	18.5	46.0	>100	
24	11.5	25.0	>100	

2. We assume that the object density was similar for all the cases listed in Table 6.3. Thus the effective area of the display was in each case proportional to the number of objects.

3. The observers knew the length of time they had in which to search the display. We assume that as a general rule they tried to cover the display uniformly in this time.

What we did with this data, then, was to suppose that the display area, A_D, in square arc-minutes was proportional to the product of the number N_o of objects and the area A_T of the objects:

$$A_D = K_1 \times N_o \times A_T$$

Inspection of images of some of the displays suggested that K_1 might be about 20.

We supposed that the glance area A_G was equal to

$$A_G = A_D/(3T_S)$$

where T_S is the search time. Finally, we assigned a value for scene complexity by trial and error; a value of $K = 0.015$ (used in the expression for F_4) was chosen. These assumptions were sufficient to calculate the probability of detection for each of the cases in Table 6.3 in which the contrast was less than unity. We have

$$SI = [F_1 \cdot F_2 \cdot F_3 \cdot F_4]^{1/2}$$

$$F_1 = 160$$

$$F_2 = \frac{M^2}{M^2 + 100}$$

where M is target diameter in minutes of arc,

$$F_3 = \frac{C}{0.9C + 0.1}$$

where C is target-background contrast

$$F_4 = \frac{A_T}{KA_G + (1 - K)A_T}$$

$$= \frac{1}{K\,\frac{K_1 N_o}{3T_S} + (1 - K)}$$

$$= \frac{1}{0.1\,\frac{N_o}{T_S} + 0.985}$$

The resulting value of SI was used to compute P in the usual way; no further consideration was given to the logical implications of the search process. Table 6.4 gives the probabilities so computed. If the experimental results had been reproduced exactly, each entry would have been 0.6. There is some spread in the computed results, which tend to run a little higher than 0.6. However, we find it remarkable that the probabilities computed in this way are reasonably consistent over such wide ranges of all the variables.

6.3.7 Contrast Effects During Target Search

Another aspect of the Boynton experiments may be noted. Boynton presents data showing how the probability of detection in search is affected if only the target-background contrast is varied. In our terms, this means that F_2 and F_4 (and F_1, of course) are held constant and the contrast is changed to vary F_3 and thus SI, which is then used to calculate the detection (i.e., recognition) probability. Figure 6.6 shows a set of curves obtained in this way, each one calculated by determining the value of the product $F_1F_2F_4$ which would give the proper value of SI for $C = 1$. Also shown are the points measured by Boynton; clearly such contrast effects are well represented by OBOE.

TABLE 6.4

CALCULATED PROBABILITY OF CORRECT TARGET
RECOGNITION FOR CONDITIONS GIVEN IN TABLE 6.3

Exposure Time, seconds	Approximate Angle Subtended by Target, arc-minutes			
	12.9	8.1	5.4	4.05
	16 Objects			
3	0.77	0.89	0.65	----
6	0.79	0.82	0.75	0.54
12	0.81	0.76	0.76	0.58
24	0.77	0.74	0.76	0.61
	64 Objects			
3	0.72	0.60	----	----
6	0.85	0.84	0.56	----
12	0.85	0.80	0.72	----
24	0.87	0.83	0.78	0.51
	256 Objects			
3	----	----	----	----
6	0.60	----	----	----
12	0.76	0.60	----	----
24	0.90	0.81	----	----

6.3.8 Display Search Experiments

In various experiments Erickson[7] has studied the ability of a subject to locate a Landolt-C on fixed and moving displays containing a number of annuli identical to the C except for the absence of a gap. One of the results was data on the mean time to search fixed displays as a function of the number of objects on the display. Data is shown in Fig. 6.7. In the experiments the targets were 0.5 inches in diameter and the display was 2 feet square. The targets subtended 17.9 arc-minutes at the

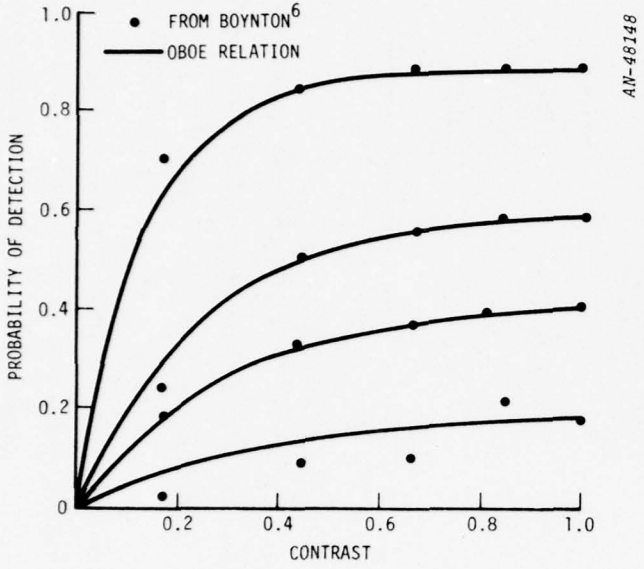

Figure 6.6. Probability of Correctly Detecting (Recognizing) Target as a Function of Contrast

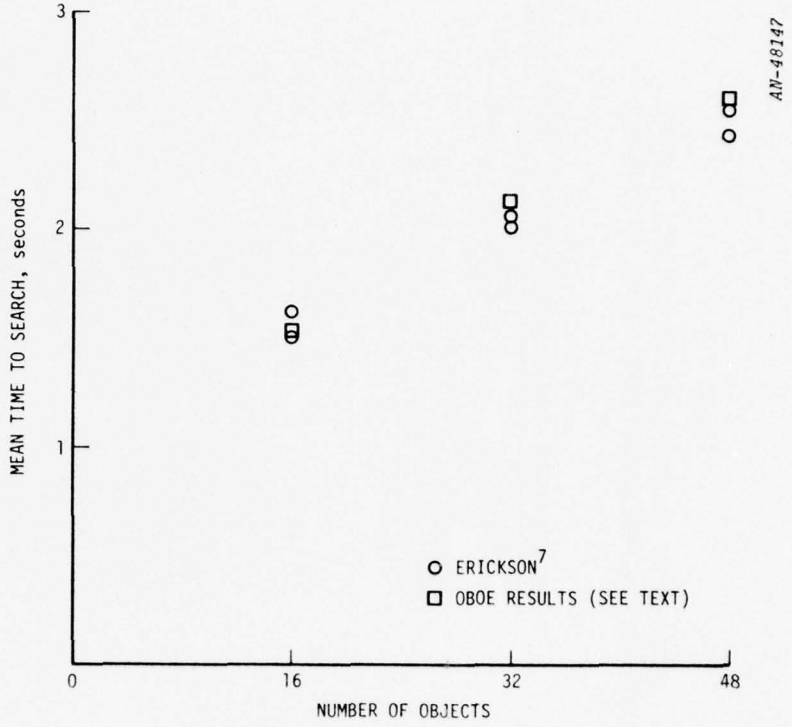

Figure 6.7. Mean Time to Search as a Function of Number of Objects on Display

eye of the observer, and the target background contrast was 0.95. Inspection of images of the displays suggested that when 48 targets were displayed the complexity appeared to be perhaps on the order of that in the Boynton experiments, so we supposed that for 48 targets, K in F_4 could again be set equal to 0.015.

For a given glance area, A_G, we thus have

$$SI = \left\{ 160 \times \frac{17.9^2}{17.9^2 + 100} \times \frac{0.95}{0.9 \times 0.95 + 0.1} \times \frac{1}{0.015 \frac{A_G}{A_T} + 0.985} \right\}^{1/2}$$

If P is the probability computed from this value of SI, the mean time to search (MTS) the display would be (for quasi-uniform search)

$$MTS = \frac{A_D/A_T}{A_G/A_T} \cdot \frac{2 - P}{6P}$$

We varied A_G to find the minimum MTS, under the assumption that the observer functions in an optimum way, and obtained a minimum MTS for $A_G/A_T \simeq 250$ of 2.59 seconds, a value which agrees well with the plotted points in Fig. 6.7. When fewer objects appear on the display in this case the density is lower, since the display area is held fixed. We found that if we made the complexity proportional to the number of objects, we did not get a good match to the data in Fig. 6.7. However, if we supposed that the complexity was proportional to the square-root of the number of objects (or the object density), and followed the same procedure we obtained a good match to the data, as shown by the points plotted in Fig. 6.7. Although setting the complexity equal to the square root of object density is obviously an ad hoc assumption here, it has some logical basis if it is assumed that the confusing objects can be

thought of as noise, and their contributions added in root-square. It should also be noted, however, that the reaction time of the subjects might also affect the experimental results when dealing with these rather short search times.

6.3.9 Minimum Resolvable Temperature

In representing the performance of FLIR sensors it is fairly common to employ the concept of minimum resolvable temperature. This concept associates with each spatial frequency a temperature differential. In the Night Vision Laboratory model use of the concept,[12] which we will consider here, a given target-background temperature difference thus implies a corresponding spatial frequency. This spatial frequency is compared with the dimension of the target to determine probabilities of recognition, using data like those in Table 6.1.

In order to compare the results of such a calculation with those of OBOE, we will consider a specific system and, using first the MRT calculation and then OBOE, calculate threshold target size as a function of target-background temperature differential. (The threshold target has an 0.5 probability of recognition.)

An approximate formula for minimum resolvable temperature, MRT, is

$$MRT = 0.66\bar{S}\,\frac{NE\Delta T f_o}{MTF(f_o)}\left(\frac{4}{\pi}\,\frac{\Delta x \Delta y}{\eta_{ovsc} F_R t_e}\right)^{1/2}\left(4f_o^2(\Delta x)^2 + 1\right)^{-1/4}$$

where MRT = minimum resolvable temperature associated with spatial frequency f_o

$\bar{S}$ = a threshold signal-to-noise ratio = 2.25

$NE\Delta T$ = sensor noise-equivalent temperature difference

f_o = spatial frequency, cycles/mrad

$MTF(f_o)$ = sensor modulation transfer function

$\Delta x, \Delta y$ = detector angular dimensions, mrad

η_{ovsc} = overscan ratio

F_R = frame rate

t_e = eye integration time

We consider a specific system, in which

$$NE\Delta T = 0.4°K$$

$$MTF(f_o) = \exp\left(-2\pi^2\sigma^2 f_o^2\right)$$

$$\sigma = 0.1 \text{ mrad}$$

$$\Delta x = \Delta y = 0.2 \text{ mrad}$$

$$\eta_{ovsc} = 1$$

$$F_R = 20 \text{ s}^{-1}$$

$$t_e = 0.2 \text{ s}$$

Although these values do not represent any particular system, they are more or less typical. The MTF expression chosen represents a system having an overall gaussian PSF having a standard deviation of about twice that which would result from the detector alone.

Substitution in the above equation gives

$$MRT = 0.067 f_o \exp\left(0.197 f_o^2\right)\left(0.16 f_o^2 + 1\right)^{-1/4}$$

The threshold target, which has a 0.5 probability of recognition, must subtend three cycles according to Table 6.1 (we use Relation B); hence the threshold target diameter, M , is given by

$$M = \frac{3}{f_o}$$

For a given f_o we find a target-background temperature differential from the MRT equation and a threshold target diameter from the last equation and plot these against each other as shown in Fig. 6.8.

To obtain comparable data using the OBOE formulation we proceed as follows:

The RMS displayed noise, R_1, to which the observer responds is

$$R_1 = Q \frac{NE\Delta T}{(F_R t_e)^{1/2}}$$

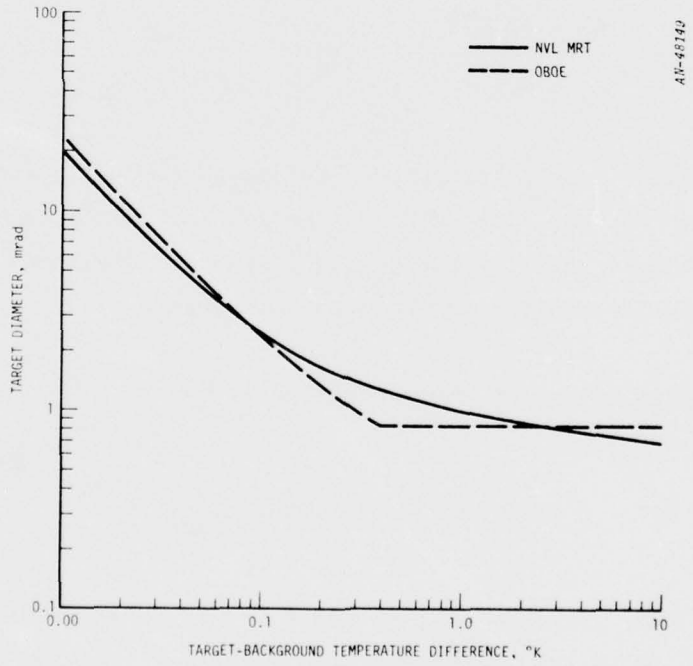

Figure 6.8. Threshold Target Diameter, Temperature Difference Relations for a Particular Sensor

where Q is a proportionality constant relating temperature differences to display brightness differences. The target-background difference signal to which the observer responds is QT_E, where T_E is the effective target-background temperature difference. If

$$2R_1 > QT_E$$

which may be written

$$\frac{2NE\Delta T}{T_E(F_r t_e)^{1/2}} > 1$$

the noise is integrated to determine the effective system resolution. We assume that this noise has a Wiener spectrum $V(k_1,k_2)$ having the form

$$V(k_1,k_2) = V_o \exp\left[-4\pi^2\eta^2\left(k_1^2 + k_2^2\right)\right]$$

The bandwidth of the displayed noise is usually wider than the system frequency response, since the optical blur and the detector area contribute to the latter and not to the former. Hence we assume that

$$\eta = \sigma/\sqrt{2}$$

where as before σ represents the standard deviation of the PSF of the system. Here again the assumptions about the spectrum of the displayed noise are arbitrary but represent the simplest reasonable assumptions.

In the OBOE formulation, when the noise is smoothed, the effective RMS noise, R_2, will be

$$R_2 = \sqrt{\frac{\eta^2}{\eta^2 + S^2}} \cdot R_1$$

$$= \sqrt{\frac{\sigma^2}{\sigma^2 + 2S^2}} \cdot Q \frac{NE\Delta T}{(F_R t_e)^{1/2}}$$

and S must be chosen so that

$$R_2 = 0.5QT_E$$

where T_E is the effective target-background temperature difference. When S is chosen in this way, the effective system resolution is characterized by a PSF having the standard deviation $\sqrt{\sigma^2 + S^2}$. If the target is displayed with high contrast, the threshold target diameter, M, must satisfy the following relation derived from the OBOE expression for SI :

$$M = 3.33\sqrt{2\pi}\sqrt{\sigma^2 + S^2}$$

Taken together, the last three equations yield the relation

$$M = 3.33\sqrt{\pi}\sigma\left[1 + \frac{4NE\Delta T^2}{T_E^2 F_R t_e}\right]^{1/2}$$

This equation applies as long as the last term in the bracket is greater than unity; when it is smaller no integrating of the noise is required, and

$$M = 3.33\sqrt{2\pi}\sigma$$

For a given T_E , M can be calculated from the last two equations, using the values of the constants given earlier. The results are also plotted in Fig. 6.8. It can be seen that OBOE and the MRT formulation give rather similar results in this case.

7 PROGRAM INPUT AND OUTPUT DESCRIPTIONS

7.1 INPUTS

The inputs to IOTA were designed for ease in preparation and modification. They are markedly different from those for GAMMA, which emphasized flexibility at the expense of ease in preparation. The inputs required fall into the following categories:

1. General Input Data
2. Sensor-Specific Data (FLIR or TV and LLTV)
3. Sensor MTF Data
4. Cumulative Probability Mode Data

The types of data needed for each category are presented in detail in Tables 7.1 through 7.7. It can be seen from Table 7.1 that the General Input Data include the identify of the type of sensor being modeled, a variety of geometrical factors (target coordinates and dimensions, aircraft position and velocity, sensor pointing direction display/observer geometry), and external world descriptors such as the scene complexity factor, and the atmospheric visibility.

The FLIR Sensor-Specific Data (Table 7.2) include descriptors of the target and background, the atmospheric extinction coefficient and sensor descriptor data for each of the FLIR modules (optics, detector, amplifier, and display). The target and background data include the target/background temperatures and spectral emissivities.

The TV and LLTV Sensor-Specific Data (Table 7.4) include data on scene illumination, spectral reflectivities for the target and the background, spectral transmittance and sensor descriptor data for each of the TV or LLTV modules (Optics, Aperture Stop, Intensifier, TV Camera, Amplifier and Display).

The Sensor MTF Data for each sensor (Tables 7.3 and 7.5) include the MTF data for each of the sensor modules being modeled.

TABLE 7.1

GENERAL INPUTS DATA FOR FLIR, TV, OR LLTV

QD( )	Data	Units	Value	Input
1	Sensor type		(see Note 1)*	
2	Target X-coordinate	ft		
3	Target Y-coordinate	ft		
4	Target Z-coordinate	ft		
5	Target dimension, side	ft		
6	Target dimension, front	ft		
7	Target dimension, height	ft		
8	Target orientation angle	deg	(see Note 2)	
9	Aircraft location X-coordinate	ft		
10	Aircraft location Y-coordinate	ft		
11	Aircraft location Z-coordinate	ft		
12	Aircraft velocity X-coordinate	ft/s	(see Note 3)	
13	Aircraft velocity Y-coordinate	ft/s	(see Note 3)	
14	Aircraft velocity Z-coordinate	ft/s	(see Note 3)	
15	Sensor depression	deg		
16	Sensor offset	deg		
17	Sensor horizontal field	deg		
18	Display height	ft		
19	Display width	ft		
20	Display-observer distance	ft		
21	Scene complexity		(see Note 4)	
22	Visibility	ft		

*Notes to this series of tables follow Table 7.7.

TABLE 7.2

ADDITIONAL FLIR INPUTS

QD( )	Data	Units	Value	Input
23	Target temperature	°K		
24	Background temperature	°K		
25	Minimum background temperature	°K		
26	Maximum background temperature	°K		
27	Number of wavelengths	real	N_1	
N_1 entries	Wavelength values	μm		
N_1 entries	Atmospheric extinction	ft^{-1}		
N_1 entries	D*	$cm \cdot Hz^{1/2}/W$		
N_1 entries	Target emissivity			
N_1 entries	Background emissivity			
N_1 entries	Emissivity, minimum background			
N_1 entries	Emissivity, maximum background			
	(OPTICAL SYSTEM) ($M_1 = 28 + 7N_1$)			
	(OPTICS)			
M_1	Horizontal field		(see Note 5)	
$M_1 + 1$	Focal ratio			
$M_1 + 2$	Transmittance			
	(DETECTOR)			
$M_1 + 3$	Detector size, scan direction	mm		
$M_1 + 4$	Detector size, perpendicular	mm		
$M_1 + 5$	Horizontal field	mm	(see Note 5)	
$M_1 + 6$	Field rate	s^{-1}		
$M_1 + 7$	Number of scan lines	real		
$M_1 + 8$	Aspect ratio		(see Note 6)	
$M_1 + 9$	Detector time constant	s		
$M_1 + 10$	Use ratio		(see Note 7)	
$M_1 + 11$	Number of detectors	real		
	(AMPLIFIER)			
$M_1 + 12$	Frame rate	s^{-1}		
$M_1 + 13$	Number of lines	real		
$M_1 + 14$	Use ratio		(see Note 7)	
$M_1 + 15$	Minimum output		(see Note 8)	
$M_1 + 16$	Maximum output		(see Note 8)	

TABLE 7.2 (Contd.)

QD( )	Data	Units	Value	Input
	(DISPLAY)			
M_1 + 17	Horizontal field		(see Note 5)	
M_1 + 18	Minimum brightness	ft·lamberts	(see Note 9)	
M_1 + 19	Maximum brightness	ft·lamberts	(see Note 9)	
M_1 + 20	Field rate	s^{-1}		
M_1 + 21	End of data		-1.	

TABLE 7.3

FLIR MTF DATA

QF( )	Data	Units	Value	Input
	(OPTICS)			
1	Number of entries	real (see Note 10)	N_2	
N_2 entries	Independent variables			
N_2 entries	Dependent variables			
	(AMPLIFIER)			
2 + $2N_2$	Number of entries	real	N_2	
N_3 entries	Independent variables			
N_3 entries	Dependent variables			
	(DISPLAY)			
3 + $2N_2$ + $2N_3$	Number of entries	real	N_4	
N_4 entries	Independent variables			
N_4 entries	Dependent variables			
4 + $2N_2$ + $2N_3$ + $2N_4$	End of data		-1.	

TABLE 7.4

ADDITIONAL TV AND LLTV INPUTS

QD( )	Data	Units	Value	Input
23	Scene illumination	ft·candles		
24	Number of wavelengths	real	N_5	
N_5 entries	Wavelength values	μm		
N_5 entries	Target reflectivity			
N_5 entries	Background reflectivity			
N_5 entries	Minimum reflectivity			
N_5 entries	Maximum reflectivity			
N_5 entries	Spectral transmittance			
N_5 entries	Quantum efficiency			
	(OPTICAL SYSTEM) ($M_2 = 25 + 7N_5$)			
	(OPTICS)			
M_2	Horizontal field		(see Note 5)	
$M_2 + 1$	Focal ratio			
$M_2 + 2$	Transmittance			
	(APERTURE STOP AND INTENSIFIER)			
$M_2 + 3$	Maximum cathode irradiance		(see Note 11)	
	(TV CAMERA TUBE)			
$M_2 + 4$	Horizontal field		(see Note 5)	
$M_2 + 5$	Field rate	s^{-1}		
$M_2 + 6$	Aspect ratio		(see Note 6)	
$M_2 + 7$	Number of lines	real		
$M_2 + 8$	Maximum SNR			
$M_2 + 9$	Maximum cathode irradiance			
	(AMPLIFIER)			
$M_2 + 10$	Field rate	s^{-1}		
$M_2 + 11$	Number of lines	real		
$M_2 + 12$	Use ratio		(see Note 7)	
$M_2 + 13$	Minimum output		(see Note 8)	
$M_2 + 14$	Maximum output		(see Note 8)	
	(DISPLAY)			
$M_2 + 15$	Horizontal field		(see Note 5)	
$M_2 + 16$	Minimum brightness		(see Note 9)	
$M_2 + 17$	Maximum brightness		(see Note 9)	
$M_2 + 18$	Field rate	s^{-1}		
$M_2 + 19$	End of data		-1.	

TABLE 7.5

TV AND LLTV MTF DATA

QF( )	Data	Units	Value	Input
	(OPTICS)			
1	Number of entries	real (see Note 10)	N_6	
N_6 entries	Independent variables			
N_6 entries	Dependent variables			
	(TV CAMERA TUBE)			
$2 + 2N_6$	Number of entries	real	N_7	
N_7 entries	Independent variables			
N_7 entries	Dependent variables			
	(AMPLIFIER)			
$3 + 2N_6 + 2N_7$	Number of entries	real	N_8	
N_8 entries	Independent variables			
N_8 entries	Dependent variables			
	(DISPLAY)			
$4 + 2N_6 + 2N_7 + 2N_8$	Number of entries	real	N_9	
N_9 entries	Independent variables			
N_9 entries	Dependent variables			
$5 + 2N_6 + 2N_7 + 2N_8 + 2N_9$	End of data		-1.	

The simpler data necessary for representing unaided vision are given in Table 7.6.

The Cumulative Probability Mode Data (Table 7.7) include a flag (1 or 0) to indicate whether this mode of calculation is desired, the time interval for printing cumulative probabilities, the time steps within each interval for performing the cumulative calculations, the speed of the aircraft, and the initial and final coordinates of the aircraft during the time being modeled.

Sample input data for a FLIR and a TV sensor are shown in Fig. 7.1. The FLIR data is contained in data arrays QD and QF, the TV data in data arrays QD2 and QF2 and the cumulative probability mode data in data array QP.

In this sample input data, in the QD array the General Input Data are contained in the first two cards, and the FLIR specific data in the next seven cards. Similarly in the QD data array the General Input Data are in the first two cards and the remaining TV sensor-specific data in the remaining ten cards.

The MTF data are contained in the QF and QF2 data arrays for the FLIR and TV sensors, respectively.

Finally data array QP shows data for a cumulative probability run with an initial sensor to target distance of 30,000 feet, a sensor altitude of 1,500 feet, a final sensor to target distance of 4,000 feet and an aircraft speed of 500 ft/s. The time interval for printing cumulative results is 2 seconds and the probability calculations are performed twice within each time interval.

Additional flexibility in running the program is provided since data can be changed in the input subroutine and the program run again.

TABLE 7.6

GENERAL INPUTS FOR UNAIDED VISION

QD( )	Data	Units	Value	Input
1	Sensor type		(see Note 1)	
2	Target X-coordinate	ft		
3	Target Y-coordinate	ft		
4	Target Z-coordinate	ft		
5	Target dimension - side	ft		
6	Target dimension - front	ft		
7	Target dimension - height	ft		
8	Target orientation angle	deg	(see Note 2)	
9	Aircraft location X-coordinate	ft		
10	Aircraft location Y-coordinate	ft		
11	Aircraft location Z-coordinate	ft		
12	Aircraft velocity X-coordinate	ft/s	(see Note 3)	
13	Aircraft velocity Y-coordinate	ft/s	(see Note 3)	
14	Aircraft velocity Z-coordinate	ft/s	(see Note 3)	
15	Radius of area searched	ft	(see Note 12)	
16 - 20	Not used			
21	Scene complexity		(see Note 4)	
22	Visibility	ft		
23	Scene illumination	ft·candles		
24	Number of wavelengths	real	N_5	
N_5 entries	Wavelength values	μm		
N_5 entries	Target reflectivity			
N_5 entries	Background reflectivity			
N_5 entries	Minimum reflectivity			
N_5 entries	Maximum reflectivity			

TABLE 7.7

CUMULATIVE PROBABILITY MODE DATA

(A) No accumulation

QP ( )		
1		0.
2	End of data	-1.

(B) Aircraft moved by AIRFLY, probabilities accumulated

QP ( )		
1		1.
2	Print interval, s	
3	Ratio of print interval to computation interval	
4	Aircraft speed, ft/s	
5 to 3N + 4	XYZ-coordinates of N successive flight path points	
3N + 5	End of data	-1.

Aircraft moved with input data and probabilities accumulated

QP ( )		
1		2.
2	Accumulation interval	
3	Constant	1.
4	= 1. if accumulation throughout run = 0. if starts anew at each calculation time	
5	End of data	-1.

NOTES TO TABLES 7.1-7.7

Note 1. 1. = FLIR, 2. = TV, 3. = LLTV, 4. = Unaided vision.

Note 2. Orientation angle is angle between plane of front of target and positive X-axis, measured counterclockwise. 0. means looking at side if view is along positive X-axis.

Note 3. Velocity vector is used only as a reference to determine sensor pointing direction. Magnitude has no effect in program.

Note 4. This dimensionless quantity is currently under examination. Values between 0.001 and 0.015 seem appropriate, with 0.005 representing "moderate" complexity and 0.01 representing "rather high" complexity.

Note 5. When "horizontal field" is specified, units are those of the corresponding MTF dominator. For example, if the MTF independent variable for one element of the optical system is cycles per milliradian, F must be given in milliradians for this part of the optical system. For the FLIR "Detector" F must be in millimeters.

Note 6. Aspect ratio is always dimension across scan divided by dimension along scan.

Note 7. Use ratio is unity minus the fractional dead time for the system.

NOTES TO TABLES 7.1-7.7 (Contd.)

Note 8. To represent optimum system performance these values should correspond numerically to those for minimum and maximum display brightness.

Note 9. Currently the magnitude of these numbers of arbitrary; however their ratio must represent the dynamic range of the display.

Note 10. The number of MTF entries for a particular component may be one or any larger integer.

Note 11. This number should agree with the corresponding TV camera tube value.

Note 12. For unaided vision it is assumed that a fixed, more-or-less circular area of the ground is searched.

```
*
      PROGRAM IOTA
*
*     GENERAL RESEARCH CORPORATION PROGRAM IOTA
*     CONTACT  A. STATHACOPOULOS OR M. GILMORE   805-964-7724
*
000003       COMMON /PRINTOU/ KPOPT
000003       COMMON/OPER/OO(200),OF(200),OP(200)
000003       DIMENSION OO2(200),OF2(200)
000003       DATA OO/
     +  1.,   0.,0.,0.,21.,10.,8.,0.,  0.,0.,1500.,500.,0.,0.,
     +  20.62,0.,.5,.,.333,1.0833,1.69,.001,6.E3,
     +  287.,295.,290.,300.,
     +   5.,7.5,8.5,9.5,10.5,11.5,
     +   1.7E-5,1.7E-5,1.7E-5,1.7E-5,1.7E-5,1.7E-5,
     +   2.4E10,2.4E10,2.4E10,2.4E10,2.4E10,
     +   .9,.9,.9,.9,.9,.9,.9,.9,.9,.9,.9,
     +  .9,.9,.9,.9,.9,.9,.9,.9,25.1,2.7,.65,.05,.05,25.1,20.,360.,
     +  .75,0.,.75,180.,20.,360.,.75,.2,10.,330.,.2,10.,20.,-1./
000003       DATA OF/
     +  7.,2.46,3.70,4.93,6.15,7.40,8.63,9.88,
     +  .9,.84,.78,.71,.65,.59,.52,
     +   7.,
     +   5.7E5,3.5E5,1.14E6,1.42E6,1.71E6,2.E6,2.28E6,
     +  .99,.99,.99,.99,.99,.97,.95,
     +   7.,
     +   .2,.4,.6,.8,1.,1.2,1.4,
     +   .95,.83,.7,.53,.37,.23,.15,-1./
000003       DATA OO2/
     +  2.,   0.,0.,0.,21.,12.,8.,0.,  0.,0.,1500.,500.,0.,0.,
     +  20.62,0.,.5,.,.333,1.0833,1.69,.001,6.E4,
     +  5.03,11.,.325,.375,.425,.475,.525,.575,.625,.675,.725,
     +  .775,.825,.06,.06,.06,.06,.07,.08,.08,.08,.08,.07,
     +  .03,.11,.17,.17,.21,.23,.23,.26,.28,.29,.32,
     +  .02,.02,.02,.02,.02,.02,.02,.02,.02,.02,.02,
     +   .4,.4,.4,.4,.4,.4,.4,.4,.4,.4,
     +  1.,1.,1.,1.,1.,1.,1.,1.,1.,1.,1.,
     +  1.,.97,.33,.67,1.,1.,.63,.33,.07,0.,0.,
     +  12.7,2.8,.05,1.E-5,12.7,
     +   31.,                    .75,525.,100.,1.E-5,30.,525.,.9,
     +  .2,10.,330.,.2,10.,30.,-1./
000003       DATA OF2/
     +4.,0.,11.31,19.69,29.52,1.,.99,.9,.1,
     +7.,0.,3.94,7.87,11.8,15.7,19.7,23.6,1.,1.,.97,.84,.68,.49,.36,
     +3.,0.,7.06,8.E6,1.,.99,0.,
     +7.,.2,.4,.6,.8,1.,1.2,1.4,.95,.83,.7,.53,.37,.23,.15,-1./
000003       DATA OP/
     +1.,2.,2.,500.,3.0E4,0.,1500.,4.0E3,0.,1500.,-1./
000003   100 CONTINUE
000004       DO 110 J=1,200
000005       OO(J)=OO2(J)
000007       OF(J)=OF2(J)
000011   110 CONTINUE
000013       KPOPT=1
000014       CALL AIRFLY
```

Figure 7.1. Iota Sample Inputs

```
000015          GO TO 300
000016          QQ(2)=        20000.
****** ************************
000017          QQ(15)=       4.28
000021          CALL AIRFLY
000022          KPRT=0
000023          QQ(2)=        18000.
000024          QQ(15)=       4.79
000026          CALL AIRFLY
000027          QQ(2)=        16000.
000030          QQ(15)=       5.37
000032          CALL AIRFLY
000033          QQ(2)=        15000.
000034          QQ(15)=       5.70
000036          CALL AIRFLY
000037          QQ(2)=        14000.
000040          QQ(15)=       6.116
000042          CALL AIRFLY
000043          IF(QQ(1).EQ.2.) GO TO 200
000045          IF(QQ(1).EQ.3.) GO TO 300
000047          GO TO 100
000050    200   CONTINUE
000050          QQ(1)=3.
000051          QQ(23)=1.E-3
000053          GO TO 100
000054    300   CONTINUE
000054          END
```

Figure 7.1. (Contd.)

In this way sequences of calculations at different ranges, with different atmospheric conditions, or with different sensors can be made with a minimal number of instructions.

7.2 OUTPUTS

The output format available in the IOTA program is illustrated in Figs. 7.2 through 7.5. Figure 7.2 is an ordered summary of the inputs used in the particular run. The summary includes a reprint of the input data arrays QD, QF, and QP. These particular arrays shown in the figure are for a TV sensor case. The second portion of this output page provides some key general input conditions used in the particular calculation that may be needed for easy reference by the user. The labels used are self-explanatory.

Figures 7.3 and 7.4 are samples of output pages 2 and 3. This portion of the output provides detailed input and calculated data for the sensor system. If desired, this type of output can be printed only once in a series of similar cases where external world (target, atmosphere, aircraft) descriptors are changed. The information is provided for each one of the modules of the particular sensor. The parameters are essentially self explanatory. For example, for the case of the TV camera the first three lines (F-number, aspect ratio, MTF data, etc.) are a reprint of input data. However, the remaining quantities are calculated values as follows:

Fitted Sigma:

The standard deviation of the PSF. Units: Same as F.

Computed Sigma X and Y:

The standard deviations of the PSF in the X- and Y-directions divided by the field width.

S/N:

The maximum camera tube signal-to-noise ratio. (An input)

```
IOTA DATA AND RESULTS

TV SENSOR

INPUT SUMMARY

QD
  2.0000E+00  0.          0.          0.          2.1000E+01  1.2000E+01  8.0000E+00  0.          1.3000E+04  0.
  1.5000E+03 -5.0000E+02  0.          0.          2.0620E+01  0.          5.0000E+00  8.3300E-01  1.0833E+00  1.6900E+00
  1.0000E-03  6.0000E+04  5.0000E+03  1.1000E+01  3.2500E-01  3.7500E-01  4.2500E-01  4.7500E-01  5.2500E-01  5.7500E-01
  6.2500E-01  6.7500E-01  7.2500E-01  7.7500E-01  8.2500E-01  6.0000E-02  6.0000E-02  6.0000E-02  6.0000E-02  7.0000E-02
  8.0000E-02  8.0000E-02  8.0000E-02  8.0000E-02  8.0000E-02  8.0000E-02  7.0000E-02  9.0000E-02  1.1000E-01  1.7000E-01
  2.1000E-01  2.3000E-01  2.3000E-01  2.6000E-01  2.8000E-01  2.9000E-01  3.2000E-01  2.0000E-02  2.0000E-02  2.0000E-02
  2.0000E-02  2.0000E-02  2.0000E-02  2.0000E-02  2.0000E-02  2.0000E-02  2.0000E-02  2.0000E-02  4.0000E-01  4.0000E-01
  4.0000E-01  4.0000E-01  4.0000E-01  4.0000E-01  4.0000E-01  4.0000E-01  4.0000E-01  4.0000E-01  4.0000E-01  1.0000E+00
  1.0000E+00  1.0000E+00  1.0000E+00  1.0000E+00  1.0000E+00  1.0000E+00  1.0000E+00  1.0000E+00  1.0000E+00  1.0000E+00
  0.          7.0000E-02  3.3000E-01  6.7000E-01  1.0000E+00  1.0000E+00  6.3000E-01  3.3000E-01  7.0000E-02  0.
  0.          1.2700E+01  2.8000E+00  9.5000E-01  1.0000E-05  1.2700E+01  3.0000E+01  7.5000E-01  5.2500E+02  1.0000E+02
  1.0000E-05  3.0000E+01  5.2500E+02  9.0000E-01  2.0000E-01  1.0000E+01  3.3000E+02  2.0000E-01  1.0000E+01  3.0000E+01
 -1.0000E+00  0.          0.          0.          0.          0.          0.          0.          0.          0.

QF
  4.0000E+00  0.          1.1810E+01  1.9690E+01  2.9520E+01  1.0000E+00  9.9000E-01  9.0000E-01  1.0000E-01  7.0000E+00
  0.          3.8400E+00  7.6700E+00  1.1800E+01  1.5700E+01  1.3700E+01  2.3600E+01  1.3000E+00  1.0000E+00  9.7000E-01
  8.4000E-01  6.8000E-01  4.9000E-01  3.6000E-01  3.0000E+00  0.          7.0000E+06  8.0000E+06  1.0000E+00  9.9000E-01
  0.          7.0000E+00  2.0000E-01  4.0000E-01  6.0000E-01  5.0000E-01  1.0000E+00  1.2000E+00  1.4000E+00  9.5000E-01
  8.3000E-01  7.0000E-01  5.3000E-01  3.7000E-01  2.3000E-01  1.5000E-01 -1.0000E+00  0.          0.          0.

QP
  1.0000E+00  2.0000E+00  2.0000E+00  5.0000E+02  3.0000E+04  0.          1.5000E+03  4.0000E+03  0.          1.5000E+03
 -1.0000E+00  0.          0.          0.          0.          0.          0.          0.          0.          0.

   A/C LOCATION (FT)   1.3000E+04   0.          1.5000E+03     A/C VELOCITY (FT/SEC)  -5.0000E+02   0.          0.
   DISPLAY SCREEN HEIGHT =   .83 FT     WIDTH =  1.08 FT     DISTANCE FROM OBSERVER TO SCREEN =   1.69 FT
   VISIBILITY(FT) =   5.0000E+04
TARGET GROUND LOCATION (FT)  0.          0.          0.
TARG SIZE (FT)  2.1300E+01  1.2000E+01  8.0000E+00    ORIENTATION (DEG)  0.          CONFUSING OBJ DENSITY -1.0000E-03
A/C - TARG RANGE (FT)  1.3086E+04    SENSOR DEPRESSION (DEG)  2.0620E+01    OFFSET  0.          F.O.V.  5.0000E+00
   WAVE LENGTH VALUES (LAMBDA)
 3.2500E-01  3.7500E-01  4.2500E-01  4.7500E-01  5.2500E-01  5.7500E-01  6.2500E-01  6.7500E-01  7.2500E-01  7.7500E-01
 8.2500E-01
   PDT 3 OF LAMBDA TABLE
 1.3000E+03  1.0000E+00  1.0000E+00  1.0000E+00  1.0000E+00  1.0000E+00  1.0000E+00  1.0000E+00  1.0000E+00  1.0000E+00
 1.0000E+00
   Q OF LAMBDA TABLE
 0.          7.0000E-02  3.3000E-01  6.7000E-01  1.0000E+00  1.0000E+00  6.3000E-01  3.3000E-01  7.0000E-02  0.
 0.
   TARGET REFLECTIVITIES (RHO T)
 6.0000E-02  8.0000E-02  8.0000E-02  6.0000E-02  7.0000E-02  8.0000E-02  8.0000E-02  8.0000E-02  8.0000E-02  8.0000E-02
 7.0000E-02
   BACKGROUND REFLECTIVITIES (RHO B)
 9.0000E-02  1.1000E-01  1.7000E-01  1.7000E-01  2.1000E-01  2.3000E-01  2.3000E-01  2.6000E-01  2.8000E-01  2.9000E-01
 3.2000E-01
   FT-CANDLES =  5.0000E+03
```

Figure 7.2. Iota Sample Output--Page 1

```
. SENSOR SYSTEM

   OPTICS

   F =  1.2700E+01

   MTF INDEPENDENT VARIABLE VALUES
1.          1.1810E+01  1.9690E+01  2.9520E+01

   MTF DEPENDENT VARIABLE VALUES
1.0000E+00  9.9000E-01  9.0000E-01  1.0000E-01

   FITTED SIGMA =  7.7004E-03

   COMPUTED SIGMA X =  6.0636E-04     SIGMA Y =  6.0636E-04

   FF =  2.8000E+00     TAU =  9.5000E-01

   APERTURE STOP

   MAXIMUM IRRADIANCE =  1.0000E-05

   TV CAMERA TUBE

   F =  1.2700E+01     ASPECT RATIO =  7.5000E-01     NO. OF LINES =  5.2500E+02

   MTF INDEPENDENT VARIABLE VALUES
1.          3.9400E+00  7.8700E+00  1.1800E+01  1.5700E+01  1.9700E+01  2.3600E+01

   MTF DEPENDENT VARIABLE VALUES
1.0000E+00  1.0000E+00  9.7000E-01  8.4000E-01  6.8000E-01  4.9000E-01  3.6000E-01

   FITTED SIGMA =  9.2389E-03

   COMPUTED SIGMA X =  7.2744E-04     SIGMA Y =  9.2411E-04

   S/N =  1.0000E+02     B SUB M =  1.0000E-05     FRAMES INTEGRATED =  1.0000E+00

   COMPUTED N =  3.6839E-20     ETA X =  7.2744E-04     ETA Y =  4.0299E-04

   MAX TRANSFER FUNCTION VALUE =  1.0000E-05

   AMPLIFIER

   FIELD RATE =  3.0000E+01     NO OF LINES =  5.2500E+02     USE RATIO =  9.0000E-01

   MTF INDEPENDENT VARIABLE VALUES
1.          7.0000E+05  8.0000E+05

   MTF DEPENDENT VARIABLE VALUES
1.0000E+00  9.9000E-01  0.
```

Figure 7.3. Iota Sample Output--Page 2

```
   FITTED SIGMA =  2.2768E-08

   COMPUTED SIGMA X =  4.5091E-04      SIGMA Y =  0.

   AMPLIFIER OUTPUT RANGE =  2.0000E-01,  1.0000E+01


   DISPLAY

   F =  3.0000E+02

   MIS INDEPENDENT VARIABLE VALUES
2.0000E-01  4.0000E-01  6.0000E-01  8.0000E-01  1.0000E+00  1.2000E+00  1.4000E+00

   MIS DEPENDENT VARIABLE VALUES
9.5000E-01  8.7000E-01  7.0000E-01  5.3000E-01  3.7000E-01  2.3000E-01  1.5000E-01

   FITTED SIGMA =  2.2529E-01

   COMPUTED SIGMA Y =  6.8271E-04      SIGMA Y =  6.8271E-04

   MIN TRANSFER FUNCTION VALUE =  2.0000E-01      MAX TRANSFER FUNCTION VALUE =  1.0000E+01

   FIELD RATE =  3.0000E+01      INTEGRATION TIME =  2.0000E-01
```

Figure 7.4. Iota Sample Output--Page 3

```
SYSTEM CALCULATIONS

SIGMA X HAT =  4.1323E-01     SIGMA Y HAT =  4.2895E-01     TOTAL SIGMA HAT =  4.2117E-01

D3 =  5.1464E+00     DT =  3.6144E+00

RMS NOISE =  2.4476E-02

EQUIVALENT RESOLUTION =  0.

SIGMA STAR =  1.2759E-03     SIGMA STAR HAT =  4.2117E-01

SIGMA STAR CYCLES/FRAME =  1.7640E+02

INPUT CONTRAST = -2.8048E-01

CONTRAST =  2.9769E-01     CONTRAST TRANSFER =  1.0614E+00

SIGNAL-TO-NOISE RATIO =  6.2536E+01

B1 STAR =  2.0000E-01     B2 STAR =  1.0000E+01     DYNAMIC LEVEL =  4.0040E+02

LIMITING CYCLES/FRAME =  1.7640E+02

BETA = ANGLE IN MINUTES SUBTENDED BY TARGET TO THE EYE =  3.0446E+01

MINIMUM TARGET DIMENSION ON DISPLAY =  8.8380E-03 FT


POSITION OF TARGET ON SCREEN (IN FEET) =  0.          0.

CODE CALCULATIONS
  PD(R,N) 9.9389E-01   PD(R,N,C) 9.9948E-01   PR(R,N) 1.8420E-01   PR(R,N,C) 1.1141E-01   PDXPR 1.8411E-01
  FOR COMPLEXITY = 1.0000E-03 ,
  MIN MTS,DET 1.0769E+00SEC       MIN MTS,RECOG 8.3410E+01SEC


CUMULATIVE PROBABILITIES
    COMPLEXITY    1.0000E-03
    CUMULATIVE PROBABILITY OF DETECTION    9.8451E-01
               FOLLOWED BY RECOGNITION    1.8139E-01
    CUMULATIVE PROBABILITY OF RECOGNITION    4.8014E-02
```

Figure 7.5. Iota Sample Output--Page 4

B SUB M

The maximum camera tube irradiance (on input).

Frames Integrated:

Number of frames integrated before readout (nearly always 1.0).

Computed N:

The low-frequency power spectral density of the two-dimensional noise generated by a particular element.

ETA X and Y:

Measures of the spatial bandwidth occupied by the noise.

Max. Transfer Function Value:

Upper limit on the output of a particular stage in the sensor.

Figure 7.5 is the fourth page of output and is the primary output of the model. It presents three types of overall calculated performance information; overall system performance data, OBOE display/observer performance data, and cumulative probability data if desired.

The definitions of the overall system performance descriptors are as follows:

Sigma Hat Quantities:

Overall system PSF standard deviations. Units: millimeters.

DB and DT:

Displayed background and target brightness. Units: Same as B1 STAR below.

RMS Noise:

Calculated RMS value of the spatial noise appearing on display. Units: Same as B1 STAR below.

Equivalent Resolution:

Standard deviation of the additional blur necessary to make the signal-to-noise ratio equal to 2.

Sigma STAR Quantities:

Standard deviation of system effective MTF, taking noise into account, in fractions of the field and in millimeters.

Input Contrast:

Effective target-background contrast at aperture of system.

Contrast:

Target-background contrast on the display.

Contrast Transfer:

Ratio of the two preceding quantities.

Signal-to-Noise Ratio:

Target-background difference divided by actual RMS noise.

B1 and B2 STAR:

Minimum and maximum display brightness (input values). Units: arbitrary.

Dynamic Level:

Difference between B2 STAR and B1 STAR divided by RMS noise.

Limiting Cycles/Frame:

Proportional to the reciprocal of Sigma STAR above.

BETA:

Angle subtended by displayed target at the observer's eye.

Minimum Target Dimension on Display:

Minimum target dimension size on display to be used in connection with Johnson criteria data.

Position of Target on **Screen:**

(Self explanatory)

The remaining performance data includes the effects of the observer viewing the display. The first row of data is static performance data for probabilities of detection (P_D) and recognition (P_R). Since these are static performance quantities they can be interpreted as maximum system performance limits. The factors shown in parentheses (R-resolution; N-noise; and C-contrast) are those taken into account in each particular calculation. These are explained in Sec. 5 of this report. In summary:

$P_D(R, N)$ is the probability of detection based on factors $F_1 \cdot F_2(10)$

$P_D(R, N, C)$ is the probability of detection based on factors $F_1 \cdot F_2(10) \cdot F_3$

$P_R(R, N)$ is the probability of recognition based on factors $F_1 \cdot F_2(100)$

$P_R(R, N, C)$ is the probability of recognition based on factors $F_1 \cdot F_2(100) \cdot F_3$

$P_D \times P_R$ is the product of the terms $P_D(R, N, C)$ and $P_R(R, N)$, the latter interpreted as the conditional probability of target recognition given that the target has been detected.

The next item in the output is the scene complexity index descriptor assumed for this run. The following two quantities calculated from OBOE are the minimum mean time of search for detection (MIN MTS, DET) and for recognition (MIN MTS, RECOG). Calculations of these quantities

involves factor F_4 and they are defined to mean the average time required by the observer for target detection or recognition with an optimum search procedure.

The last portion of the output format gives the cumulative probabilities of detection and recognition. As was discussed in Sec. 5, while the aircraft is moving on the prescribed flight path, at particular intervals (specified by the inputs) **the model calculates the single glance** probabilities for the displayed scene at that time; these probabilities in turn are combined as a function of elapsed time to calculate the cumulative probabilities of detection and recognition. At time intervals, also specified by inputs, the probabilities are printed out. These are:

Cumulative Probability of Detection:

This is equal to

$$1 - \prod_{i=1}^{n} (1 - P_{SGi})^k$$

where the product is taken over all calculations to the present and $k = 3 \times$ the calculation interval . P_{SGi} is the single glance detection probability, including factor F_4 .

Cumulative Probability of Detection Followed by Recognition:

The cumulative probability of detection multiplied by the single-glance probability of recognition, $P_R(R, N)$.

Cumulative Probability of Recognition:

This is the same as the cumulative probability of detection except that P_{SGi} is the single glance recognition probability, including factor F_4 .

7.3 SAMPLE

Because of the flexibility built into the output format and the modular treatment of sensors, IOTA can be used to perform different types of sensor evaluations.

- It can be used to compare FLIR, TV, and LLTV sensors.
- It can be used to evaluate sensors in terms of the displayed contrast, overall system resolution, effective overall resolution as degraded by noise and displayed signal-to-noise ratio. These can be seen in Fig. 7.6 for a TV-type sensor.
- It can be used to calculate the sensor and human observer performance limits in terms of static probabilities (Fig. 7.6).
- It can be used to calculate the sensor and human observer dynamic performance (see examples, Fig. 7.6; cumulative probabilities for two aircraft speeds).

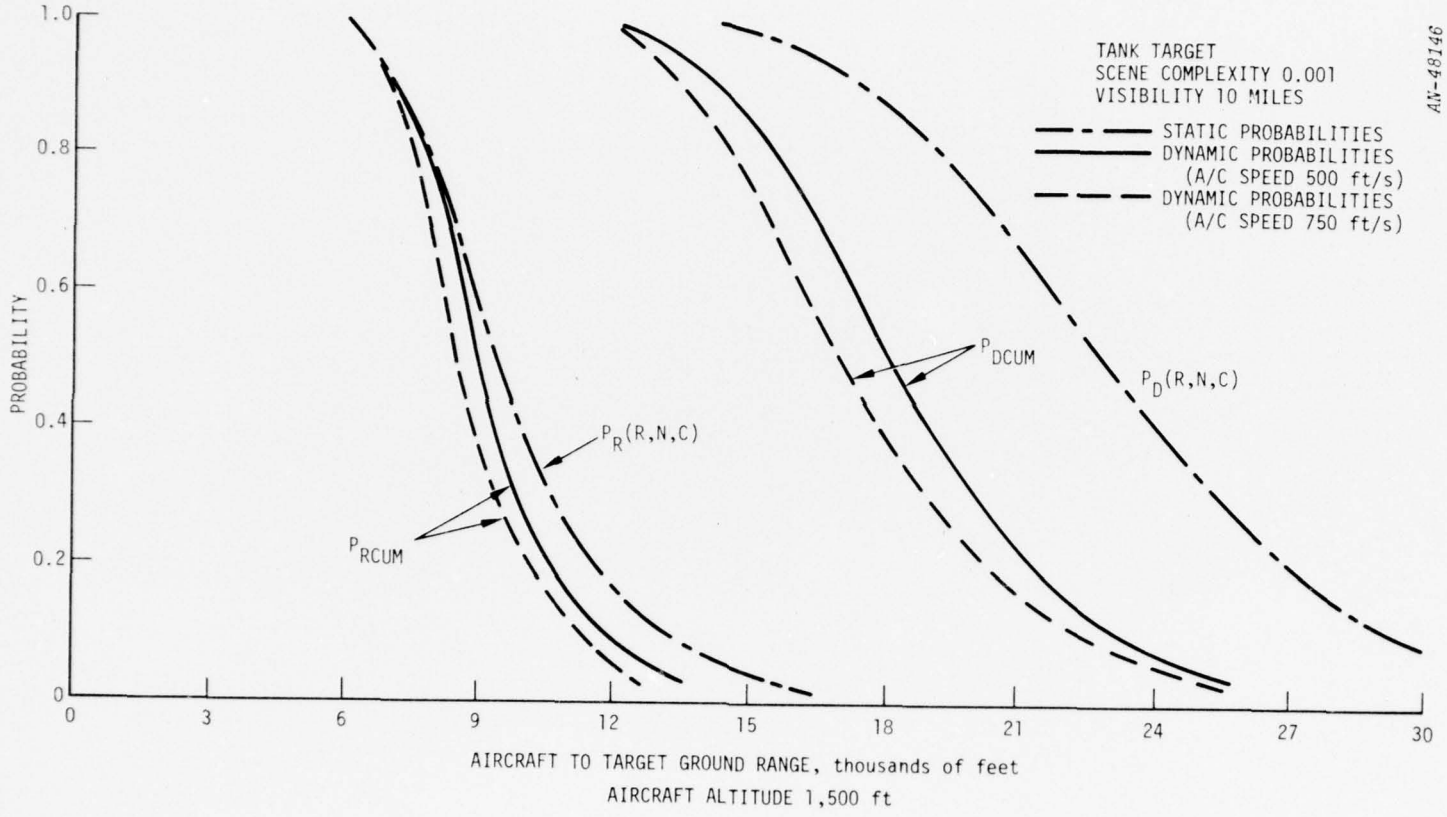

Figure 7.6. TV Sensor Performance

REFERENCES

1. A. D. Stathacopoulos et al., Review of Mathematical Models of Air-to-Ground Target Acquisition Using TV and FLIR Sensors, General Research Corporation NWC TP-5840, January 1976.

2. H. R. Blackwell, "Contrast Thresholds of the Human Eye," Journal Opt. Soc. Am., 36, 624 (1946).

3. J. Johnson, "Analysis of Image Forming Systems," Proceedings of the Image Intensifier Symposium, USA ERDL, Ft. Belvior, Virginia, October 1958.

4. F. Rosell and R. Willson, "Recent Psychophysical Experiments and the Display Signal-to-Noise Ratio Concept," Perception of Displayed Information, L. M. Biberman (ed.), Plenum Press, New York, 1973.

5. H. Bailey, Target Detection Through Visual Recognition; a Quantitative Model, The RAND Corporation RM-6158-PR, February 1970.

6. R. M. Boynton et al., Laboratory Studies Pertaining to Visual Air Reconnaissance, WADC Technical Report 55-304, April 1958.

7. R. A. Erickson, "Visual Search Performance in a Moving Structured Field," Journal Opt. Soc. Am., 54, 399, (1964).

8. A. D. Stathacopoulos et al., Computer Model for the Real-Time Night Reconnaissance/Strike Process (U), Annual Report, General Research Corporation CR-4-437, May 1968 (SECRET).

9. W. J. Smith, Modern Optical Engineering, McGraw-Hill, New York, 1966.

10. J. H. Taylor, Contrast Thresholds as a Function of Retinal Position and Target Size, SIO Ref. 61-10, Scripps Institute of Oceanography, University of California (1961).

11. V. L. Senders, "The Physiological Basis of Visual Acuity, " Psych. Bulletin, 45, 465 (1948).

12. J. O. Ratches et al., Night Vision Laboratory Static Performance Model for Thermal Viewing Systems, Army Electronics Command AD A011 212, Ft. Monmouth, New Jersey, April 1975.